Features of edge states and domain walls in chiral superconductors

Eidgenössische Technische Hochschule Zürich
Swiss Federal Institute of Technology Zurich

Manfred Sigrist

NQS2017, YITP
Kyoto

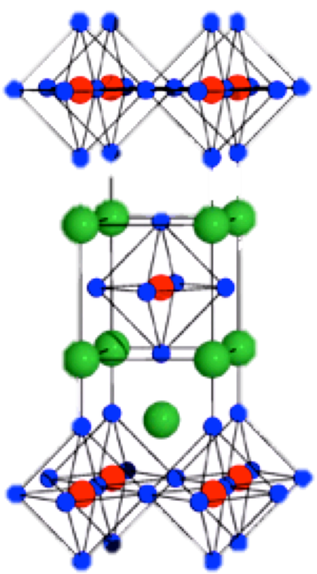

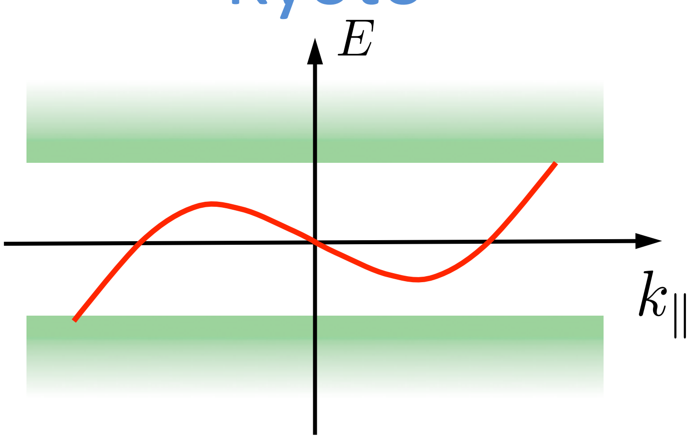

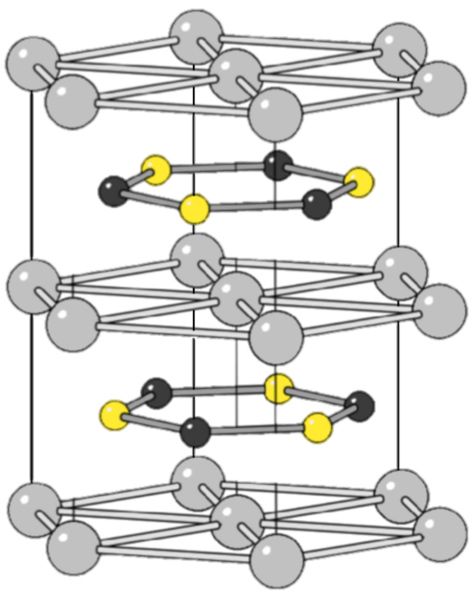

Chiral superconductors

Chiral superconductors - candidates

Sr_2RuO_4

tetragonal
crystal structure

URu_2Si_2

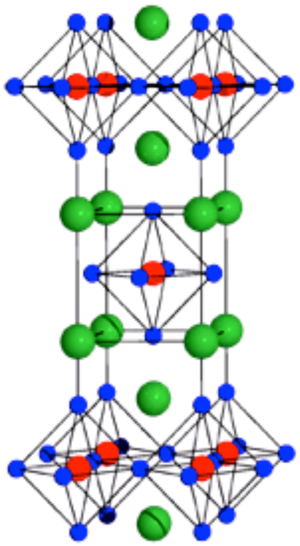

odd-parity

$$\Delta_{\vec{k}} = \Delta_0(k_x \pm i k_y)$$

chiral *p*-wave

even-parity

$$\Delta_{\vec{k}} = \Delta_0(k_x \pm i k_y) k_z$$

chiral *d*-wave

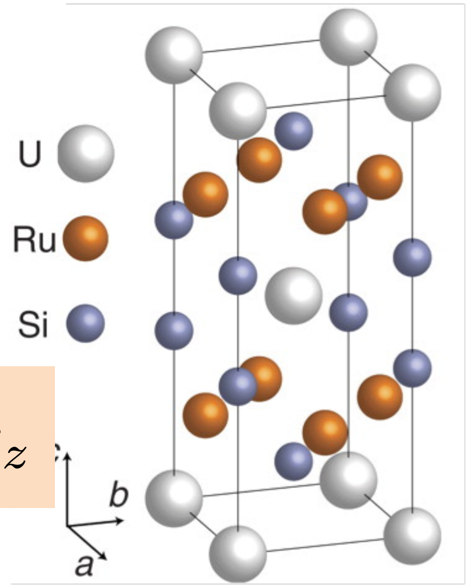

μSR
polar Kerr effect

$$\boxed{L_z = \pm 1}$$

polar Kerr effect

Chiral superconductors

Chiral superconductors - candidates

hexagonal
crystal structure

UPt$_3$

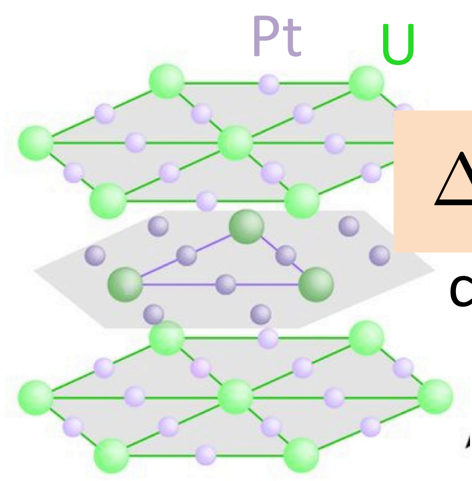

odd-parity

$$\Delta_{\vec{k}} = \Delta_0 (k_x \pm i k_y)^2 k_z$$

chiral *f*-wave

SrPtAs

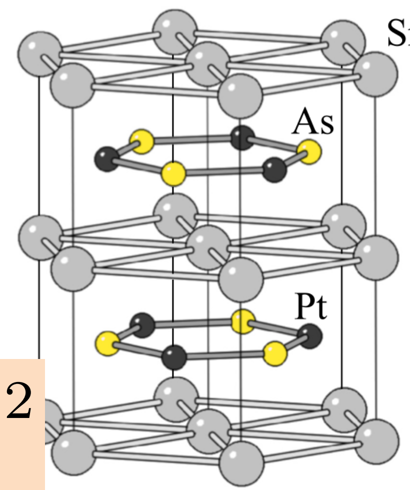

even-parity

$$\Delta_{\vec{k}} = \Delta_0 (k_x \pm i k_y)^2$$

chiral *d*-wave

μSR
polar Kerr effect

$$L_z = \pm 2$$

μSR

Content

- focus on Sr_2RuO_4 as a chiral *p*-wave SC
- edge states and edge currents in a chiral *p*-wave SC
- chiral domains

Sarah Etter

Adrien Bouhon

many other collaborators:

Y. Imai, K. Wakabayashi,
A. Furusaki, M. Matsumoto,
C. Honerkamp, M. Fischer,
T.M. Rice, J. Goryo, W. Huang, ...

former doctor students at ETH Zurich

Sr_2RuO_4

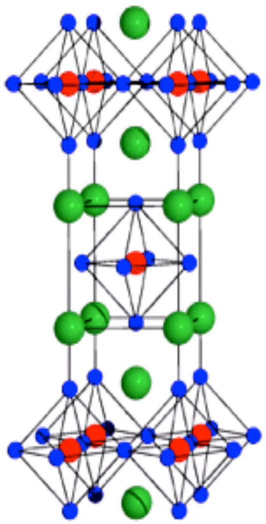

$T_c \approx 1.5K$

Maeno et al 1994

layered crystal structure

quasi-2D metal

possible odd-parity spin-triplet states

$$\hat{\Psi}(\vec{k}) = \begin{pmatrix} 0 & k_x \pm i k_y \\ k_x \pm i k_y & 0 \end{pmatrix}$$

A-phase chiral phase

pair wave function

$$\hat{\Psi} = \begin{pmatrix} \Psi_{\uparrow\uparrow} & \Psi_{\uparrow\downarrow} \\ \Psi_{\downarrow\uparrow} & \Psi_{\downarrow\downarrow} \end{pmatrix}$$

$$\hat{\Psi}(\vec{k}) = \begin{pmatrix} -k_x + i k_y & 0 \\ 0 & k_x + i k_y \end{pmatrix}$$

B-phase helical phase

Sr_2RuO_4 - chiral p-wave superconductor

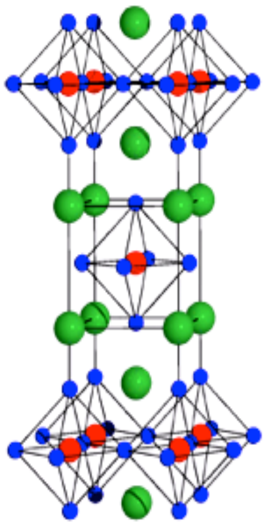

$$T_c \approx 1.5K$$

Maeno et al 1994

layered crystal structure

quasi-2D metal

$$\hat{\Psi}(\vec{k}) = \begin{pmatrix} 0 & k_x \pm i k_y \\ k_x \pm i k_y & 0 \end{pmatrix}$$

A-phase chiral phase

identifaction

- intrinsic magnetism
- inplane spin polarizable
- multi-component
- polar Kerr effect
- phase-sensitive SQUID

$$\hat{\Psi}(\vec{k}) = \begin{pmatrix} -k_x + i k_y & 0 \\ 0 & k_x + i k_y \end{pmatrix}$$

B-phase helical phase

Sr_2RuO_4 - chiral p-wave superconductor

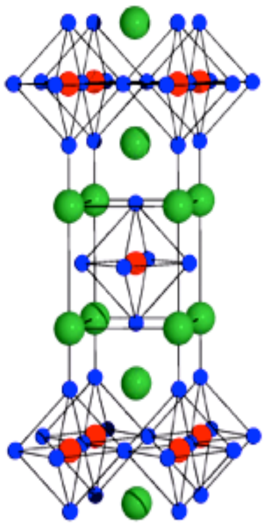

$$T_c \approx 1.5K$$

Maeno et al 1994

layered crystal structure

quasi-2D metal

$$\hat{\Psi}(\vec{k}) = \begin{pmatrix} 0 & ke^{\pm i\theta_{\boldsymbol{k}}} \\ ke^{\pm i\theta_{\boldsymbol{k}}} & 0 \end{pmatrix}$$

A-phase chiral phase

identifaction

- intrinsic magnetism
- inplane spin polarizable
- multi-component
- polar Kerr effect
- phase-sensitive SQUID

phase winding around the FS

gap function

$$\left.\begin{aligned} \Delta_{\boldsymbol{k}} &= |\Delta_0| e^{+i\theta_{\boldsymbol{k}}} \\ \Delta_{\boldsymbol{k}} &= |\Delta_0| e^{-i\theta_{\boldsymbol{k}}} \end{aligned}\right\}$$

nodeless gap

2-fold degenerate

chiral domains

chiral - broken time reversal symmetry

intrinsic magnetism in Sr_2RuO_4 ?

random local magnetism

"edge currents" around
inhomogeneities & defects

μSR - zero-field relaxtion

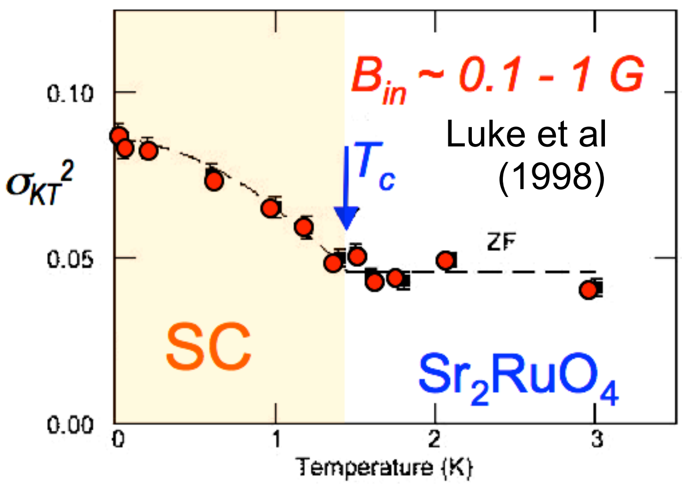

muon-spin depolarization

→ intrinsic magnetism

edge state currents

scanning probes at mesoscopic discs

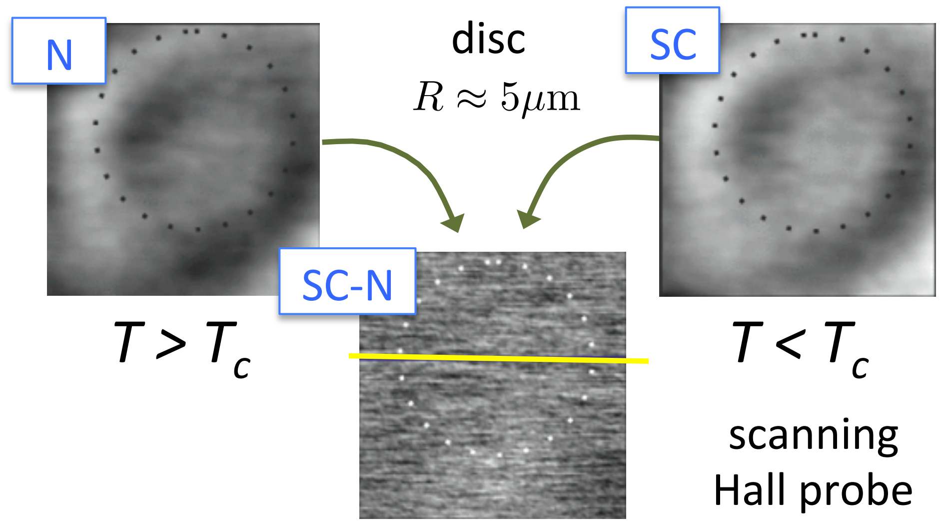

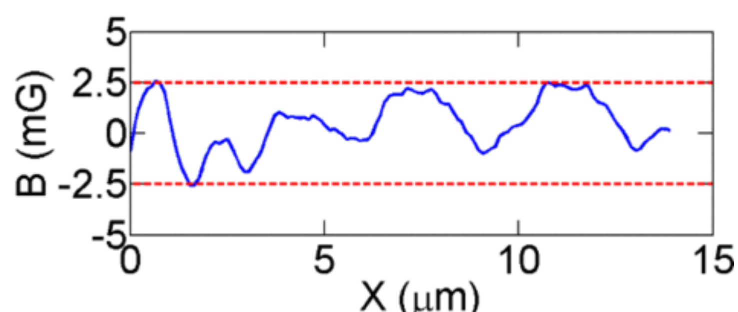

Mackenzie group (2014)

Edge currents

Sr_2RuO_4 - edge state spectrum

edge states for the chiral p-wave state

scattering of quasiparticles at the surface

solution of Bogolyubov-de Gennes equations

➡ subgap bound states (close orbits in particle-hole space)

"Andreev reflection"

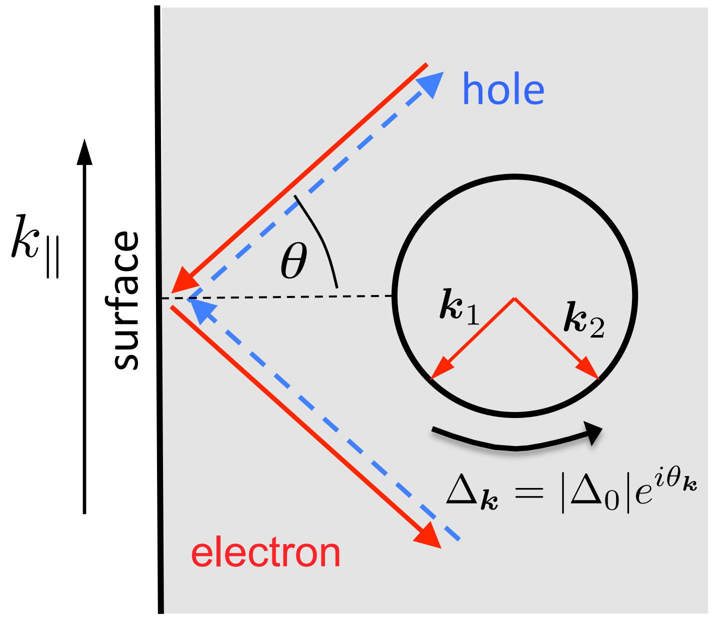

specular scattering

Bohr-Sommerfeld quantization

$$\frac{1}{\hbar} \oint \boldsymbol{p} \cdot d\boldsymbol{s} + \underbrace{\phi_{\boldsymbol{k}_1} + \phi_{\boldsymbol{k}_2}}_{\text{phase shifts at turning points}} = 2\pi n$$

for $|E| \ll |\Delta_0|$ ➡ $\phi_{\boldsymbol{k}_1} + \phi_{\boldsymbol{k}_2} = \pi + \theta_{\boldsymbol{k}_2} - \theta_{\boldsymbol{k}_1}$

$|\boldsymbol{p}| \approx \frac{E}{v_F}$ $\quad \theta_{\boldsymbol{k}_2} - \theta_{\boldsymbol{k}_1} = \pi$ ➡ $E = 0$

Sr_2RuO_4 - edge state spectrum

edge states for the chiral p-wave state

scattering of quasiparticles at the surface

solution of Bogolyubov-de Gennes equations

➡ subgap bound states (close orbits in particle-hole space)

"Andreev reflection"

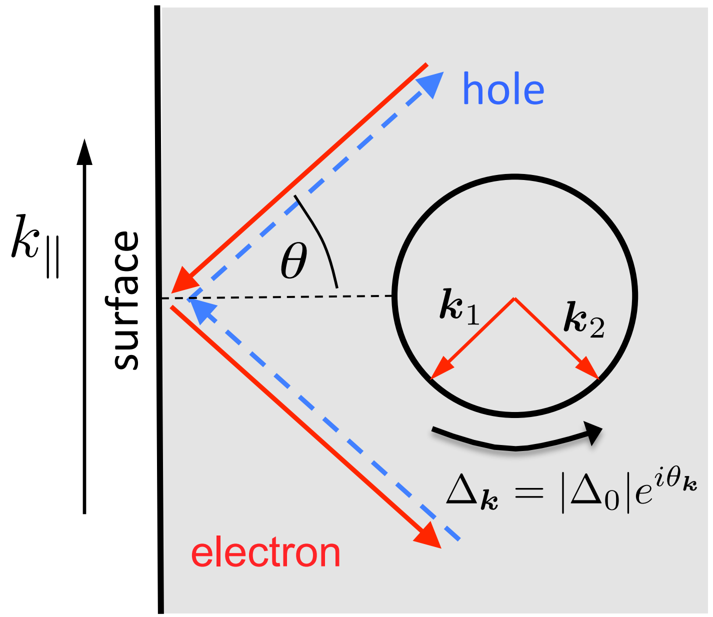

specular scattering

Bohr-Sommerfeld quantization

$$E = E_{k_{\|}} = \Delta_0 \sin\theta = \Delta_0 \frac{k_{\|}}{k_F}$$

$$2\theta = \pi - (\theta_{\vec{k}_2} - \theta_{\vec{k}_1})$$

phase shifts

Sr_2RuO_4 - bulk and edge spectrum

edge states for the chiral p-wave state

scattering of quasiparticles at the surface

solution of Bogolyubov-de Gennes equations

➡ subgap bound states (close orbits in particle-hole space)

"Andreev reflection"

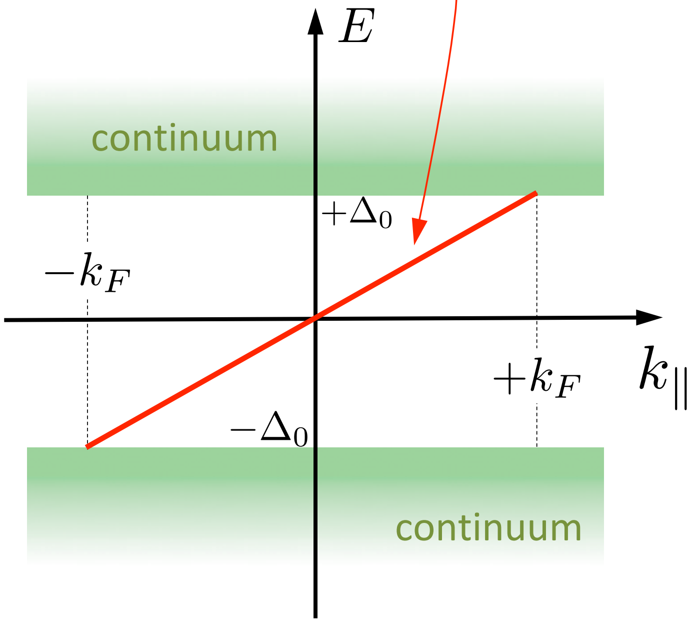

result of topological property

Bohr-Sommerfeld quantization

$$E = E_{k_{\|}} = \Delta_0 \sin\theta = \Delta_0 \frac{k_{\|}}{k_F}$$

$$2\theta = \pi - (\theta_{\vec{k}_2} - \theta_{\vec{k}_1})$$

phase shifts

note: $\theta_{\vec{k}_2} - \theta_{\vec{k}_1} = \pm\pi \longrightarrow E = 0$

Sr_2RuO_4 - bulk and edge spectrum

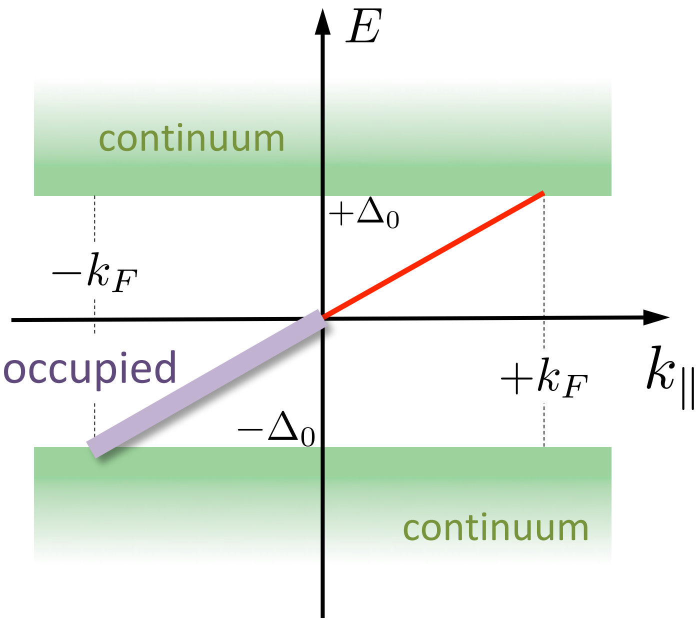

order parameter deformation

$$\Delta_{\vec{k}} = \eta_x k_x + \eta_y k_y$$

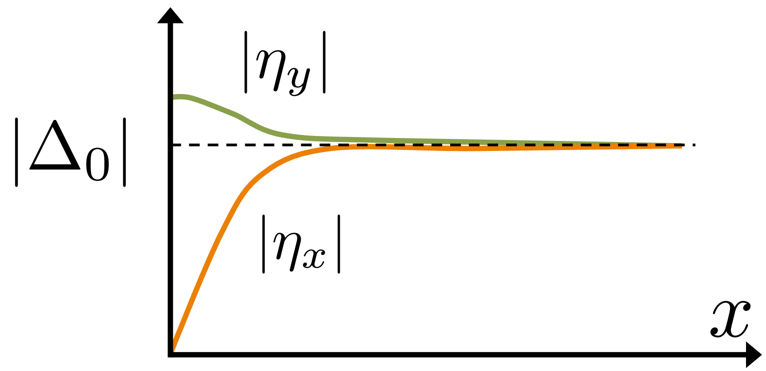

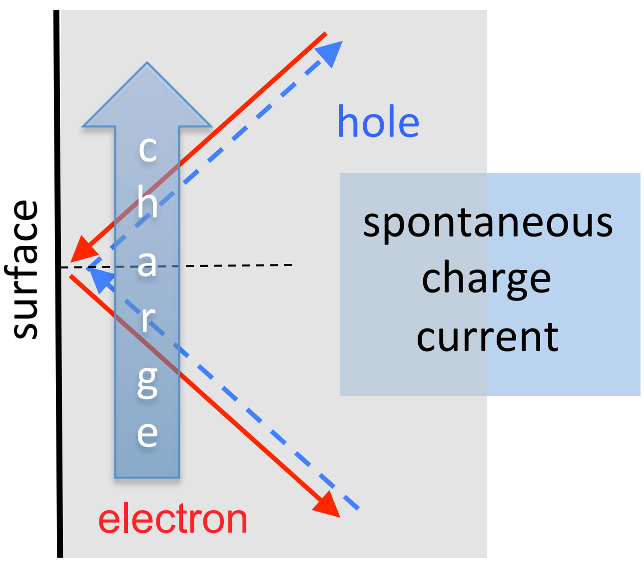

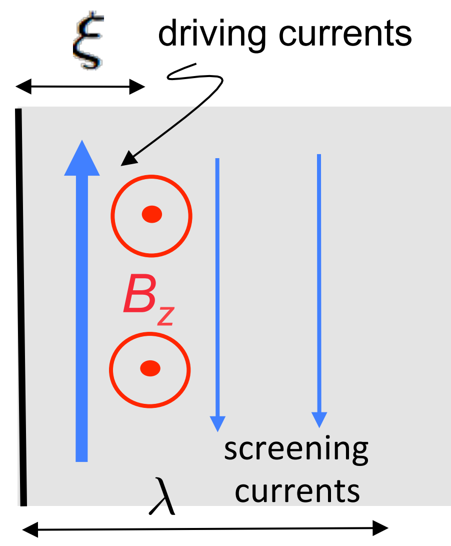

fields

$$B_z \sim 10\ \mathrm{G}$$

Topology and edge currents

Are edge currents a unique topological property?

lattice version of chiral p-wave superconductor (tight-binding):

$$\xi_{\vec{k}} = -2t(\cos k_x a + \cos k_y a) + ... - \epsilon_F$$

$$\Delta_{\vec{k}} = \Delta_0(\sin k_x a + i \sin k_y a)$$

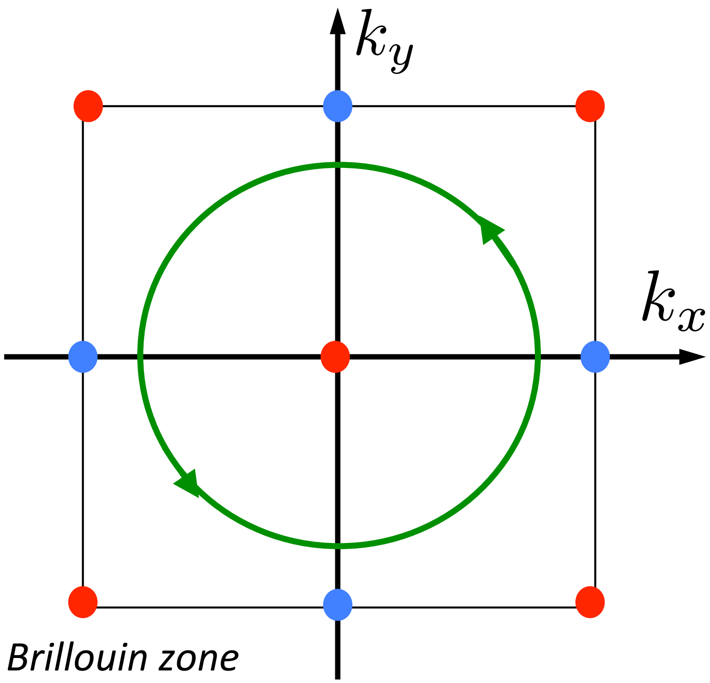

1^{st} *Brillouin zone*

zeros of $\Delta_{\vec{k}}$
- ● +1-winding
- ● -1-winding

Chern numbers

$$N = +1$$

Topology and edge currents

Are edge currents a unique topological property?

lattice version of chiral p-wave superconductor (tight-binding):

$$\xi_{\vec{k}} = -2t(\cos k_x a + \cos k_y a) + \dots - \epsilon_F$$

$$\Delta_{\vec{k}} = \Delta_0(\sin k_x a + i \sin k_y a)$$

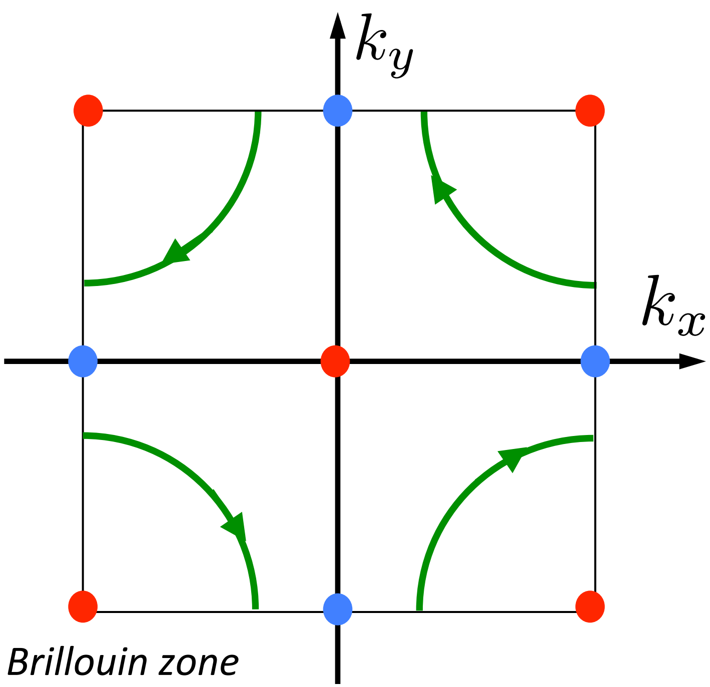

1[st] *Brillouin zone*

zeros of $\Delta_{\vec{k}}$

- +1-winding
- -1-winding

Chern numbers

$$N = +1 - 4 \times \frac{1}{2}$$

$$= -1 \times 1 = -1$$

Topology and edge currents

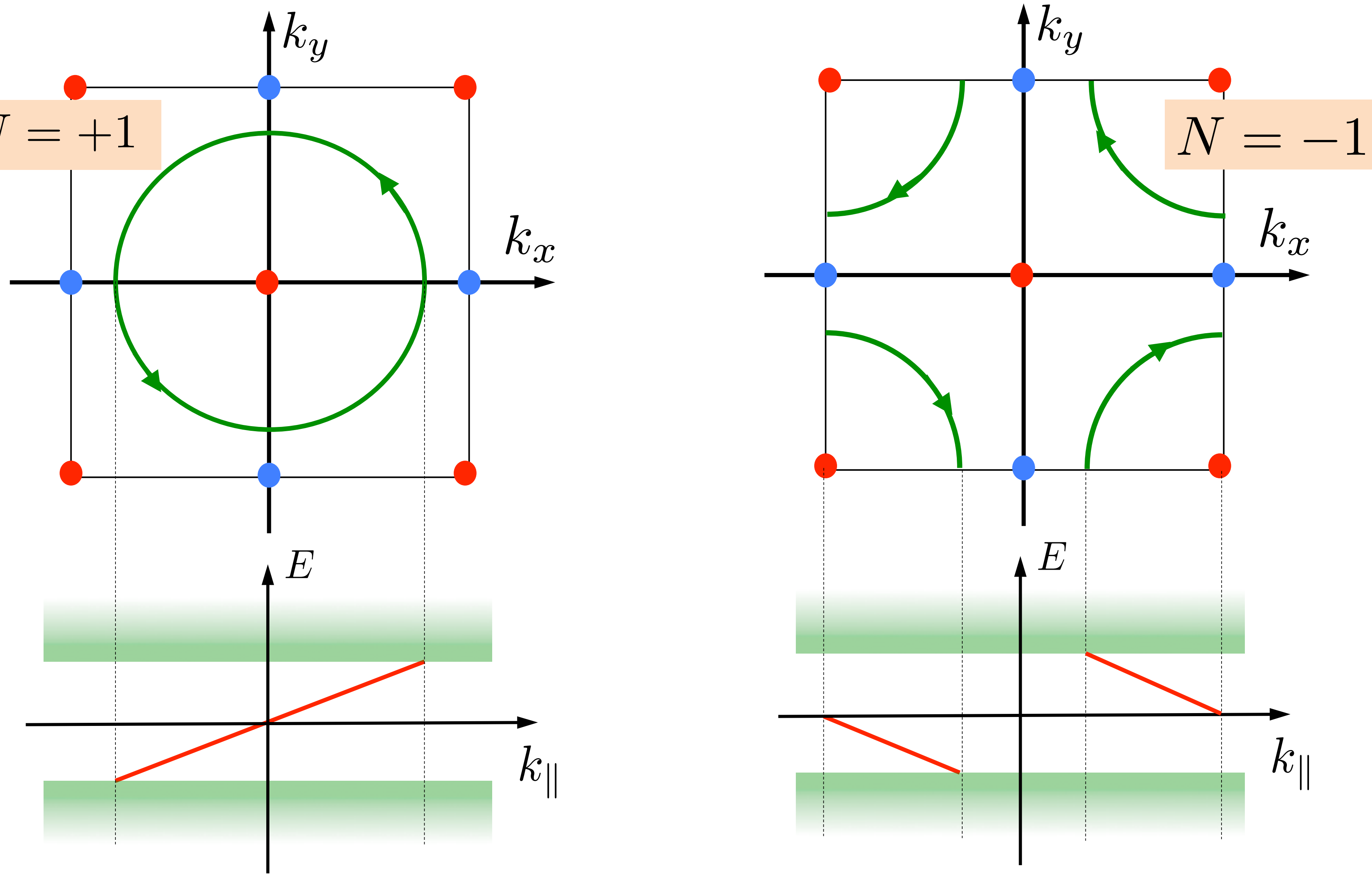

Topology and edge currents

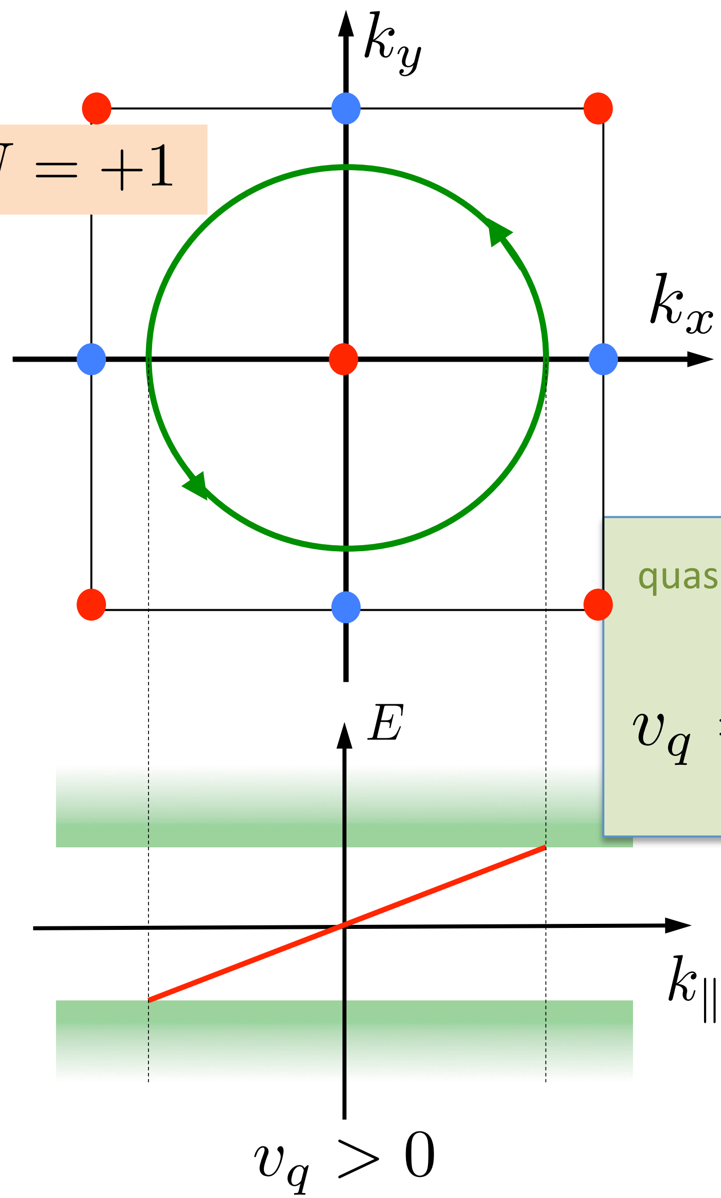

quasiparticle velocity

$$v_q = \frac{1}{\hbar}\frac{dE_{k_\parallel}}{dk_\parallel}$$

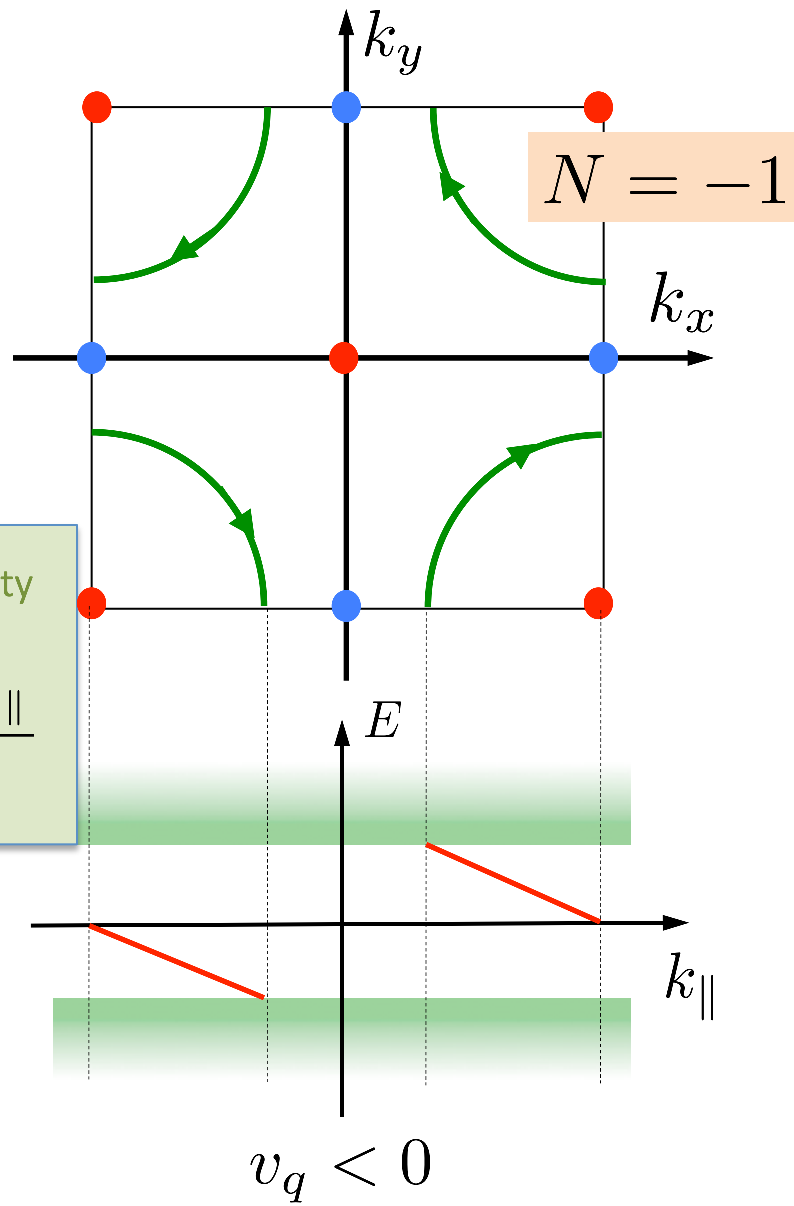

Topology and edge currents

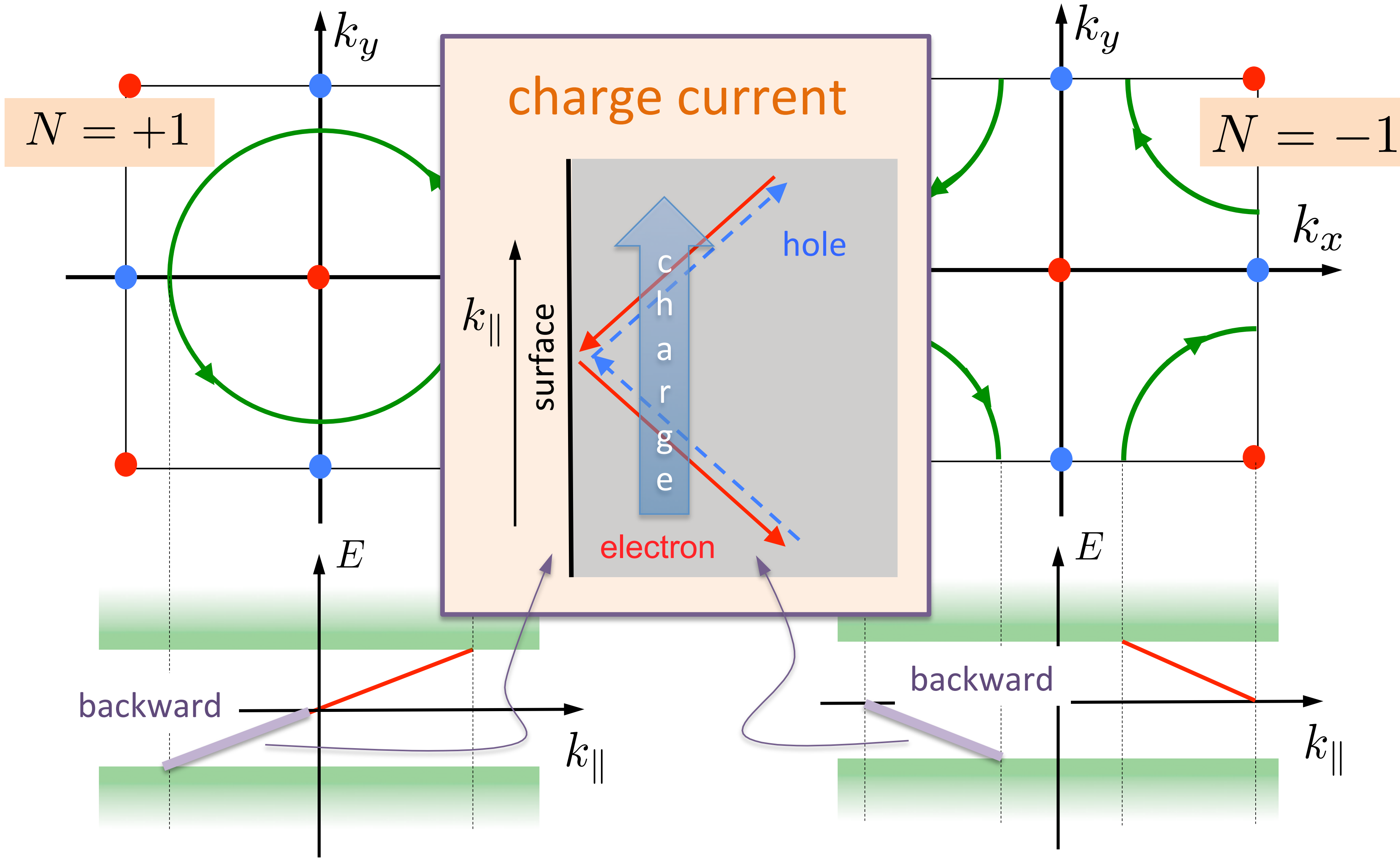

opposite chirality, but identical current direction

Topology - thermal Hall effect

“Spontaneous” Righi-Leduc effect

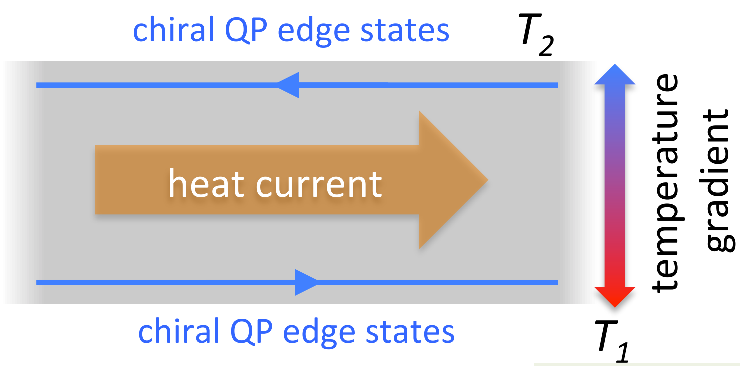

Chern number

$$\kappa_{xy} = \frac{\pi k_B^2 T}{12\hbar} N + O(e^{-\frac{\Delta}{k_B T}})$$

Read & Green; Qin, Niu & Shi; Sumiyoshi & Fujimoto; ...

property of the
(subgap) quasiparticles

$$T \ll T_c$$

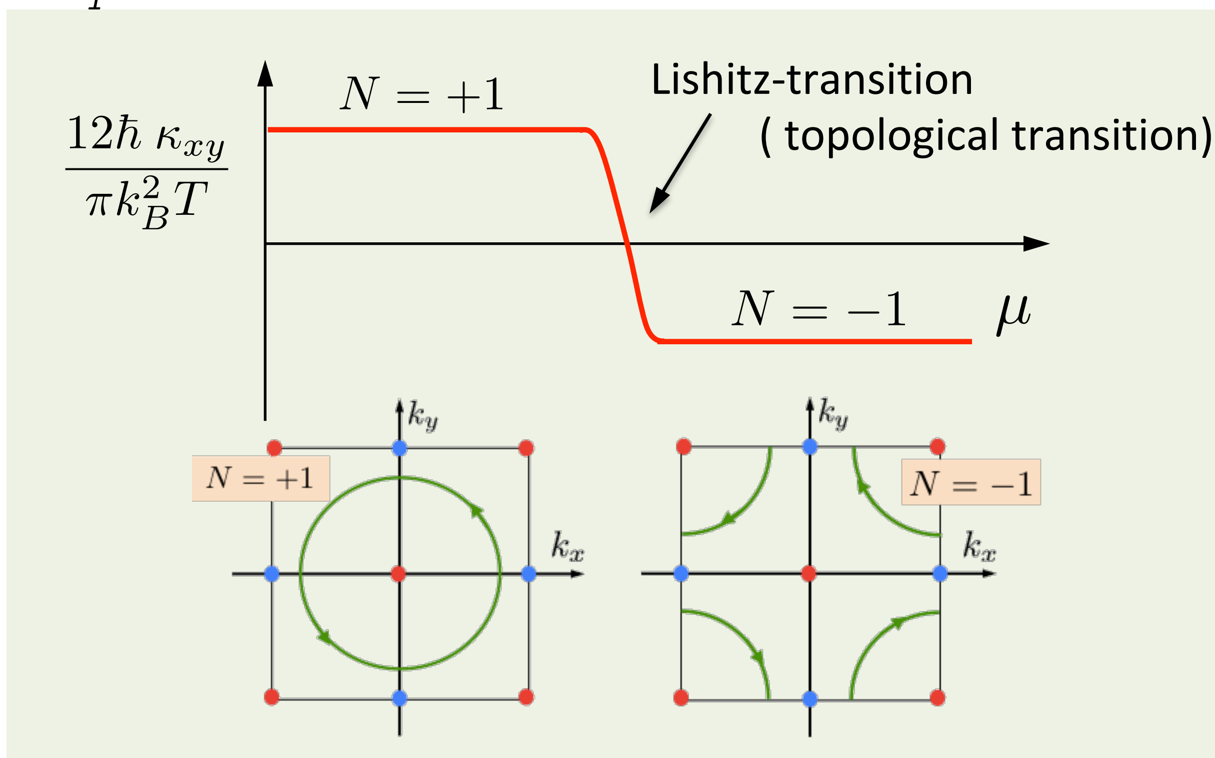

Topology - thermal Hall effect

“Spontaneous” Righi-Leduc effect

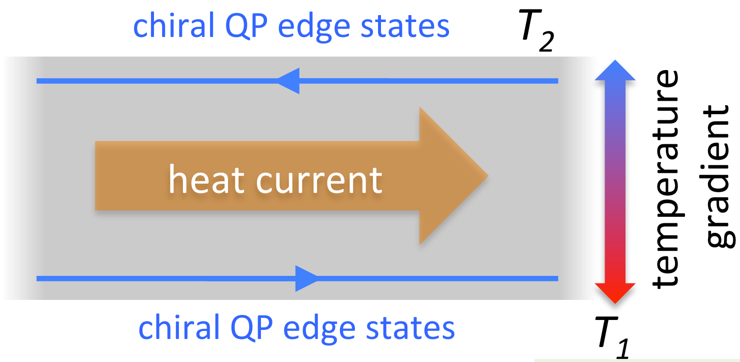

Chern number

$$\kappa_{xy} = \frac{\pi k_B^2 T}{12\hbar} N + O(e^{-\frac{\Delta}{k_B T}})$$

Read & Green; Qin, Niu & Shi; Sumiyoshi & Fujimoto; ...

property of the
(subgap) quasiparticles

$$T \ll T_c$$

analog to ν=1
Quantum Hall
effect

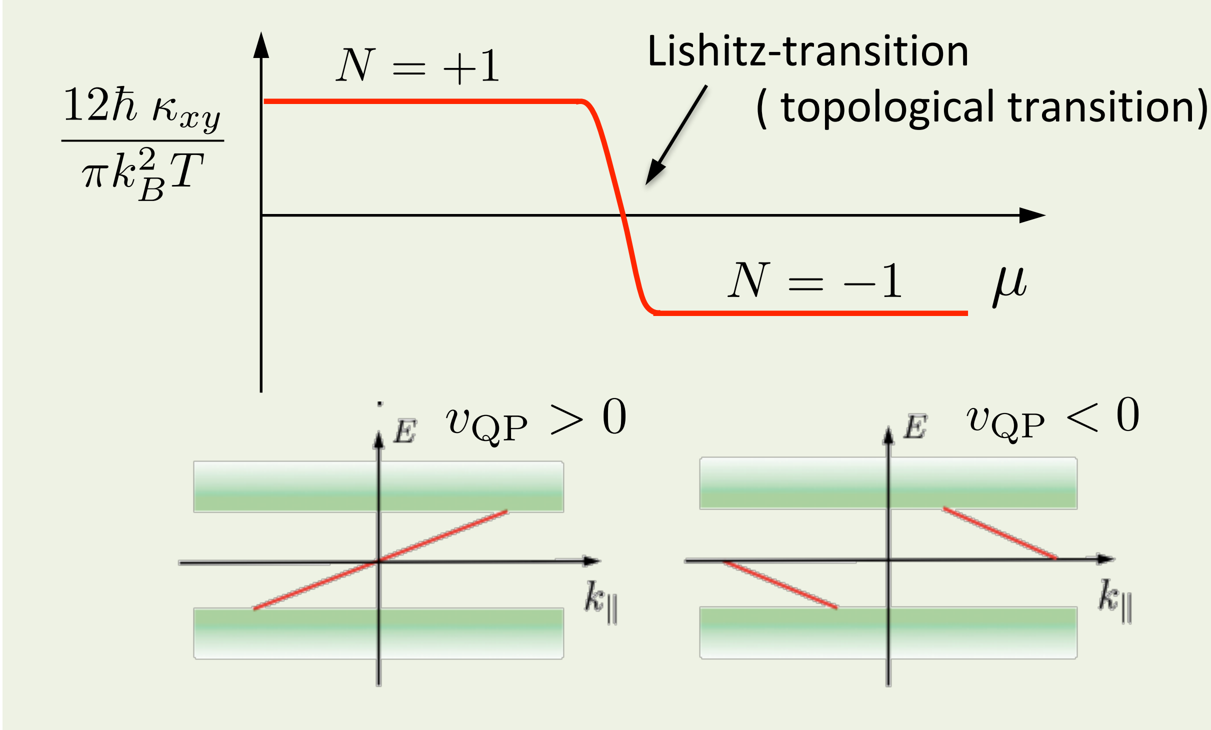

Topology and edge currents - a further twist

particle-hole symmetry

$$\Delta_{\vec{k}} = \Delta_0(\sin k_x a + i \sin k_y a)$$

$$\Delta_{\vec{k}+\vec{Q}} = -\Delta_{\vec{k}} \qquad \vec{Q} = \frac{\pi}{a}(1,1)$$

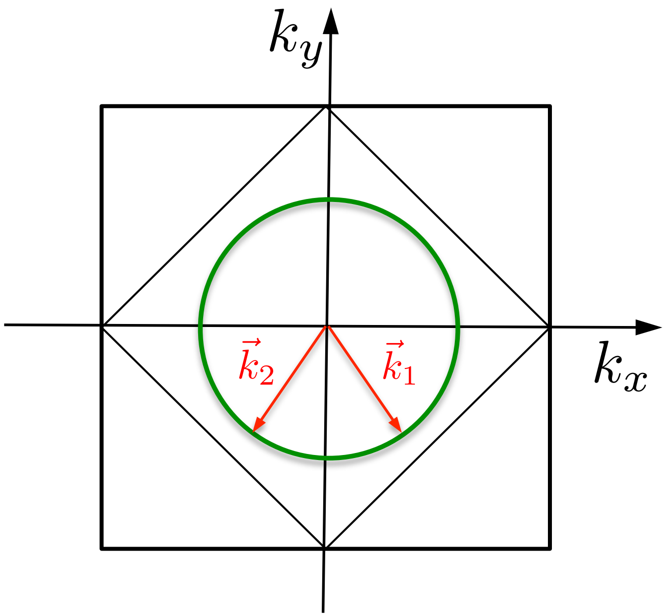

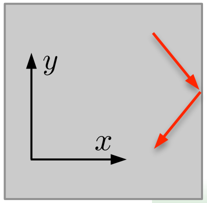

$\vec{n} = (1,0)$

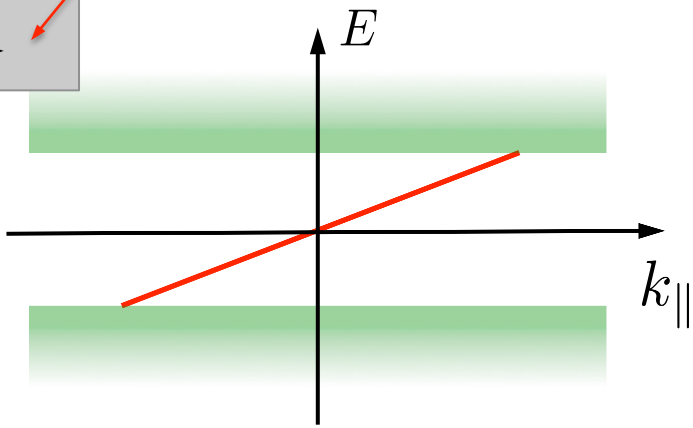

Topology and edge currents - a further twist

particle-hole symmetry

$$\Delta_{\vec{k}} = \Delta_0(\sin k_x a + i \sin k_y a)$$

$$\Delta_{\vec{k}+\vec{Q}} = -\Delta_{\vec{k}} \qquad \vec{Q} = \frac{\pi}{a}(1,1)$$

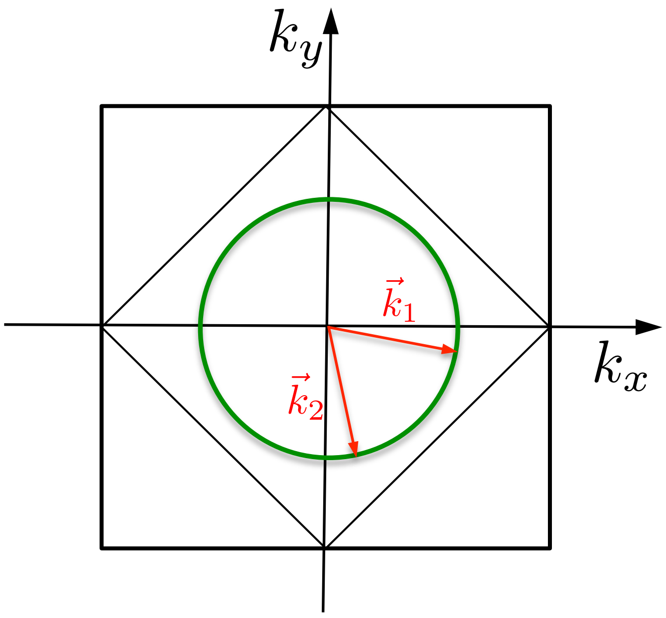

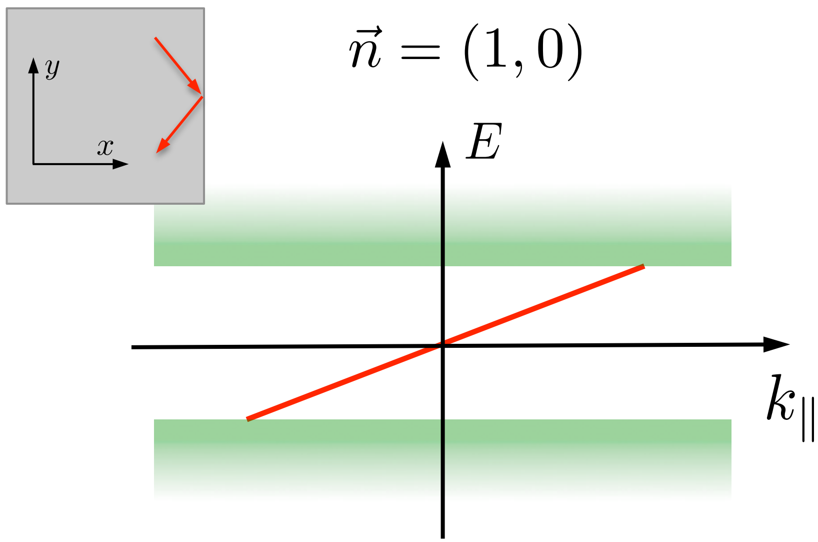

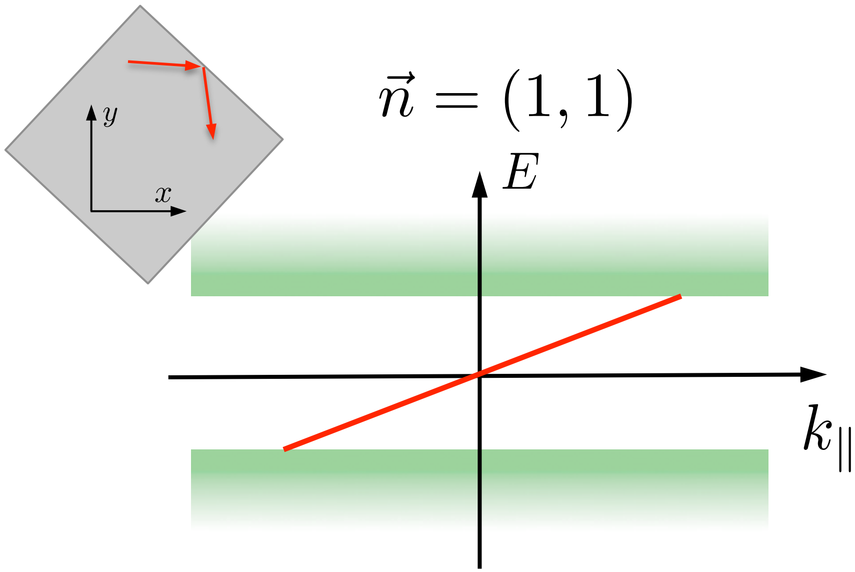

Topology and edge currents - a further twist

particle-hole symmetry

$$\Delta_{\vec{k}} = \Delta_0(\sin k_x a + i \sin k_y a)$$

$$\Delta_{\vec{k}+\vec{Q}} = -\Delta_{\vec{k}} \qquad \vec{Q} = \frac{\pi}{a}(1,1)$$

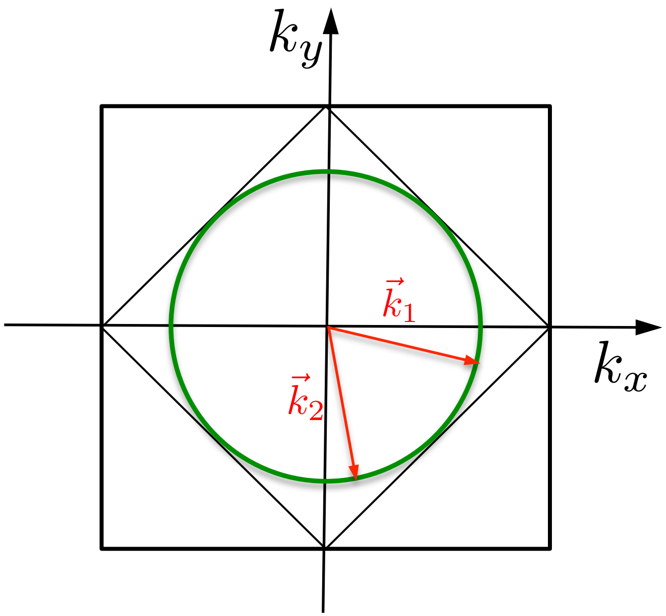

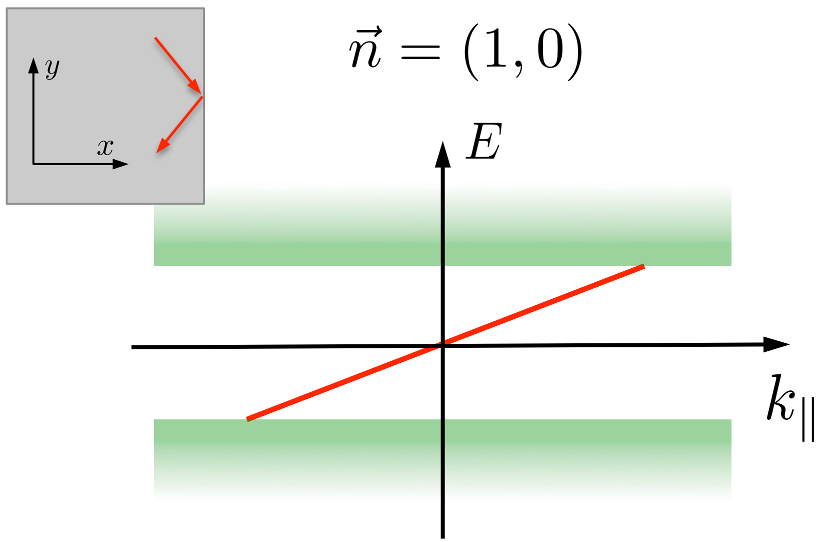

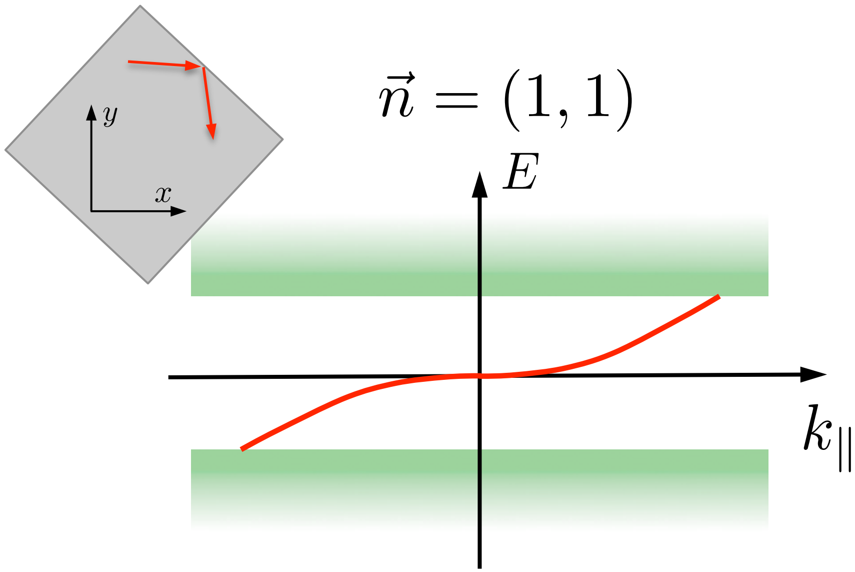

Topology and edge currents - a further twist

particle-hole symmetry

$$\Delta_{\vec{k}} = \Delta_0(\sin k_x a + i \sin k_y a)$$

$$\Delta_{\vec{k}+\vec{Q}} = -\Delta_{\vec{k}} \qquad \vec{Q} = \frac{\pi}{a}(1,1)$$

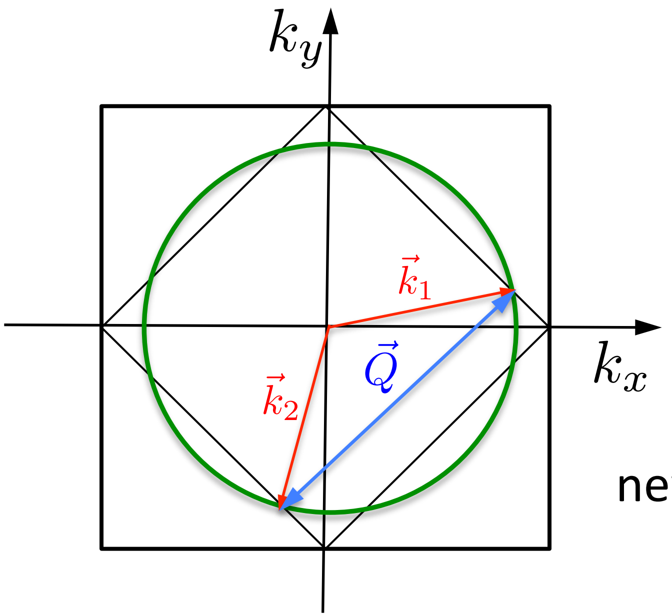

new zero-energy momenta

$$\theta_{\vec{k}_2} - \theta_{\vec{k}_1} = \pm\pi \longrightarrow E = 0$$

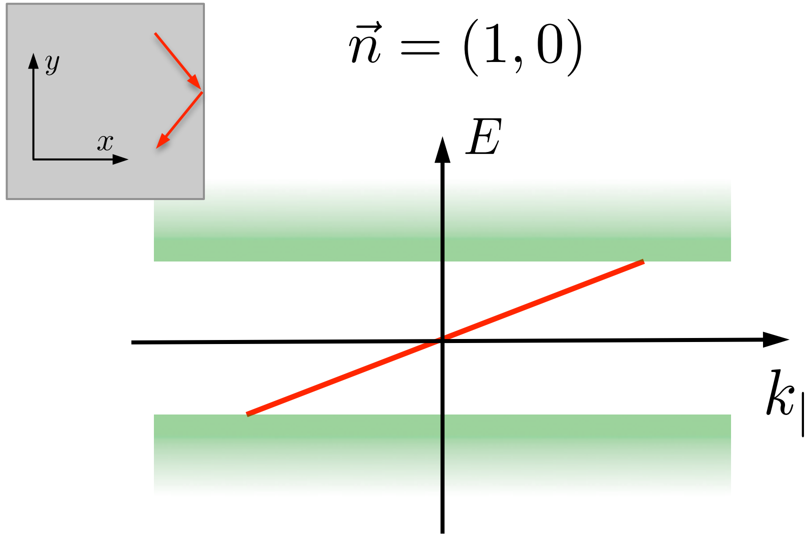

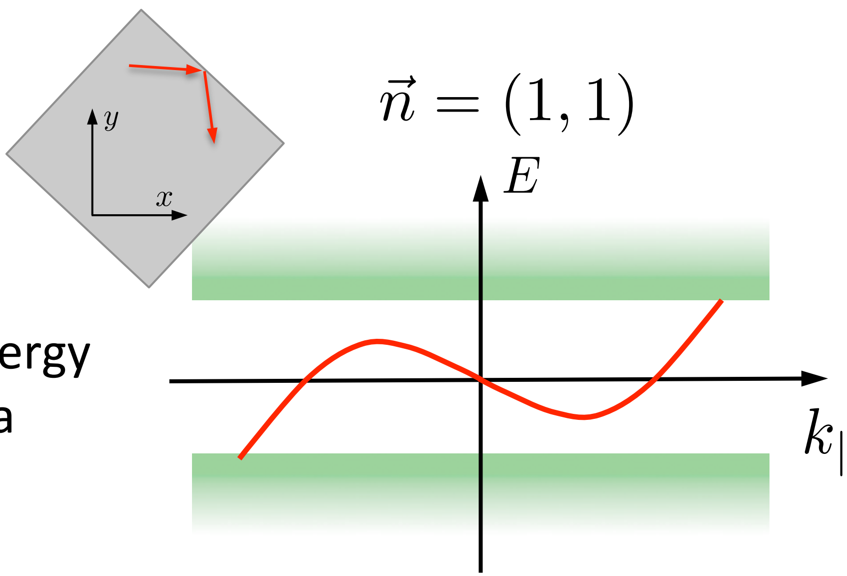

no change in Chern number

Topology and edge currents - a further twist

$$\vec{n} = (1,1)$$

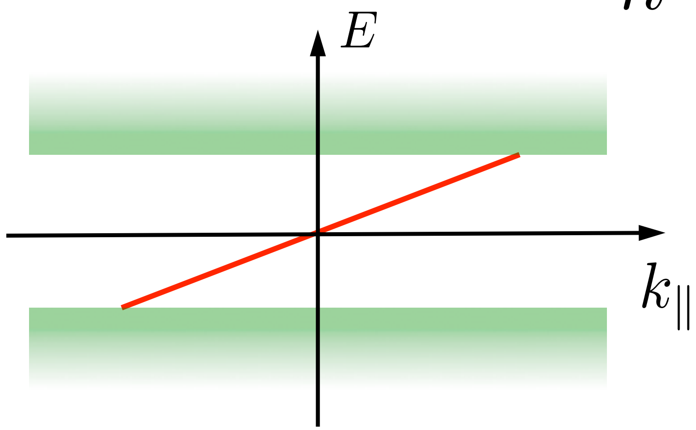

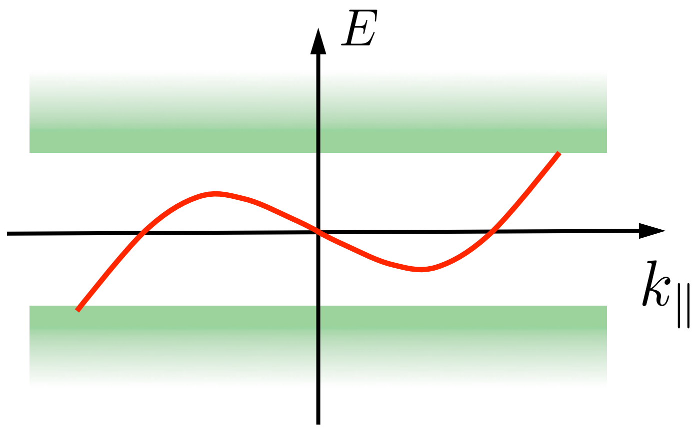

current reversal

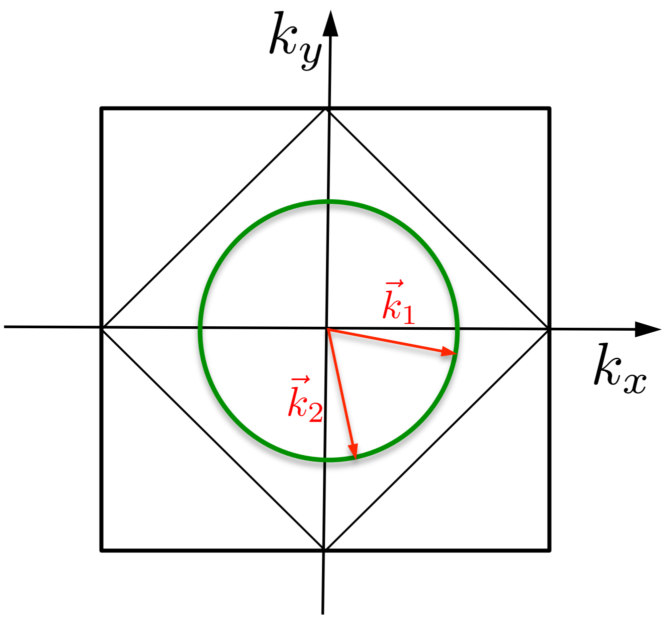

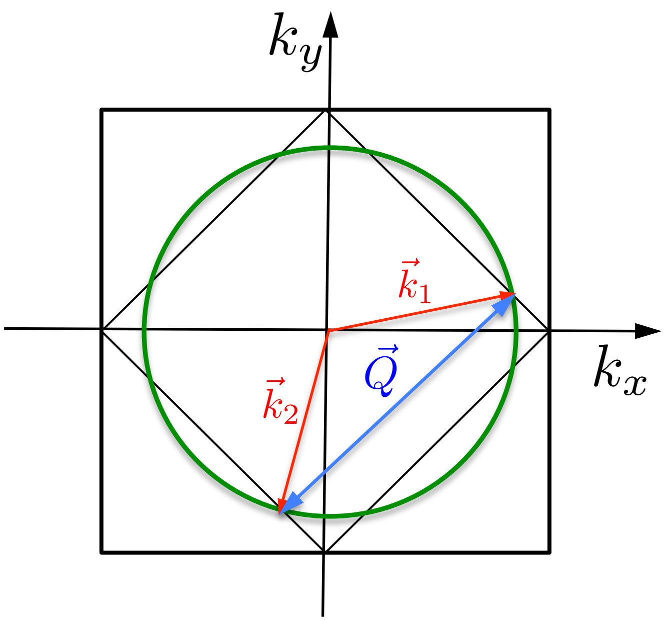

Topology and edge currents - a further twist

$$\vec{n} = (1,1)$$

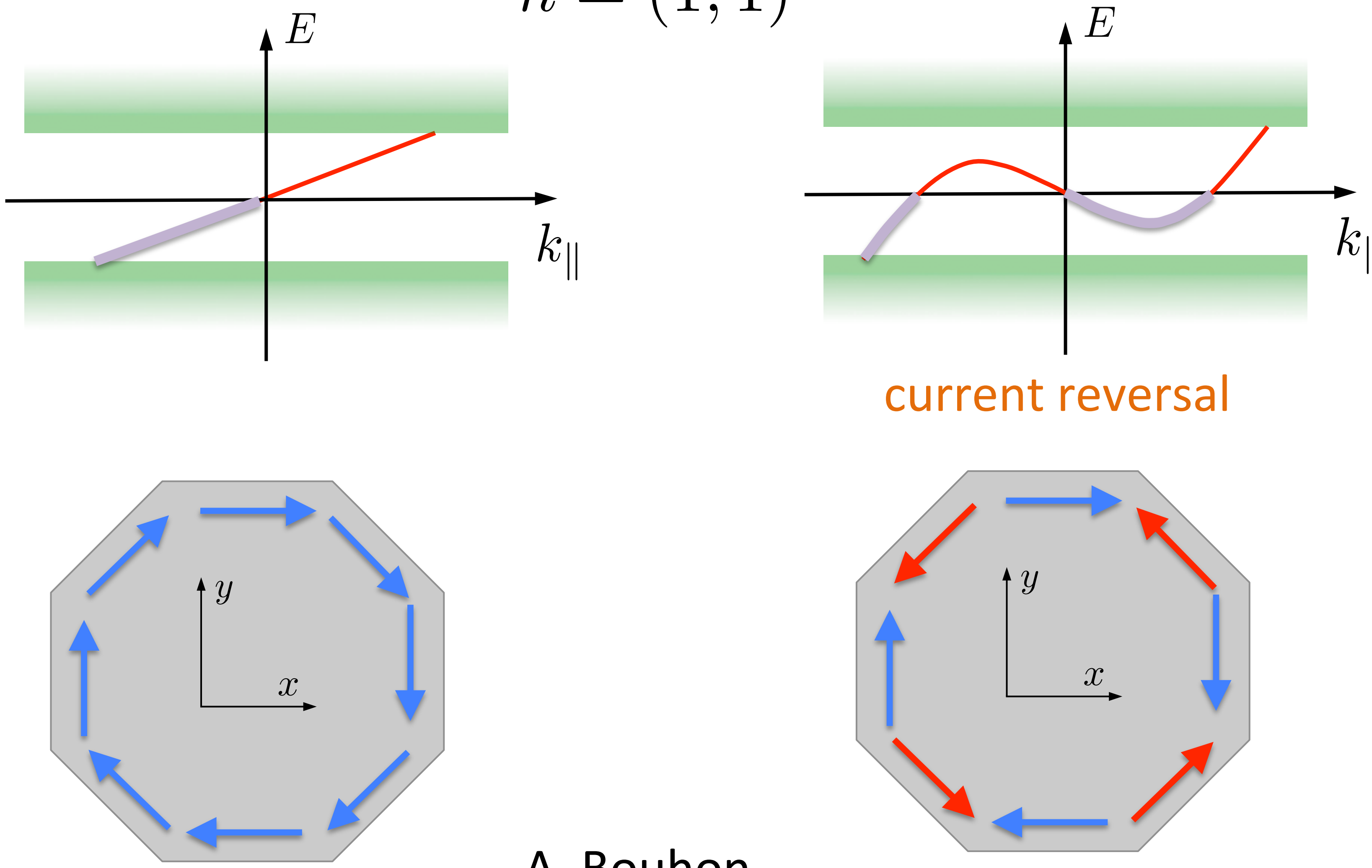

A. Bouhon

circular supercurrent

non-circular supercurrent

Ginzburg-Landau approach - chiral p-wave

order parameter: $\boldsymbol{d}(\boldsymbol{k}) = \hat{z}\boldsymbol{\eta}\cdot\boldsymbol{k} = \hat{z}(\eta_x k_x + \eta_y k_y)$

$$\mathcal{F} = \int dV \, \{a|\boldsymbol{\eta}|^2 + b_1|\boldsymbol{\eta}|^4 + b_2(\eta_x^{*2}\eta_y^2 + \eta_x^2\eta_y^{*2}) + b_3|\eta_x|^2|\eta_y|^2$$

$$+K_1(|\Pi_x\eta_x|^2 + |\Pi_y\eta_y|^2) + K_2(|\Pi_x\eta_y|^2 + |\Pi_y\eta_x|^2)$$

$$+[K_3(\Pi_x\eta_x)^*(\Pi_y\eta_y) + K_4(\Pi_x\eta_y)^*(\Pi_y\eta_x) + c.c.]$$

$$+K_5|\Pi_z\boldsymbol{\eta}|^2 + (\boldsymbol{\nabla}\times\boldsymbol{A})/8\pi\}$$

and $\boldsymbol{\Pi} = \frac{\hbar}{i}\boldsymbol{\nabla} + \frac{2e}{c}\boldsymbol{A}$

Ginzburg-Landau approach - chiral p-wave

order parameter: $\boldsymbol{d}(\boldsymbol{k}) = \hat{z}\boldsymbol{\eta} \cdot \boldsymbol{k} = \hat{z}(\eta_x k_x + \eta_y k_y)$

$$\mathcal{F} = \int dV \, \{a|\boldsymbol{\eta}|^2 + b_1|\boldsymbol{\eta}|^4 + b_2(\eta_x^{*2}\eta_y^2 + \eta_x^2\eta_y^{*2}) + b_3|\eta_x|^2|\eta_y|^2$$

$$\boxed{+K_1(|\Pi_x\eta_x|^2 + |\Pi_y\eta_y|^2) + K_2(|\Pi_x\eta_y|^2 + |\Pi_y\eta_x|^2)}$$

$$+ [K_3(\Pi_x\eta_x)^*(\Pi_y\eta_y) + K_4(\Pi_x\eta_y)^*(\Pi_y\eta_x) + c.c.]$$

$$+K_5|\Pi_z\boldsymbol{\eta}|^2 + (\boldsymbol{\nabla} \times \boldsymbol{A})/8\pi\}$$ and $\boldsymbol{\Pi} = \frac{\hbar}{i}\boldsymbol{\nabla} + \frac{2e}{c}\boldsymbol{A}$

length scales for amplitude modulations for the two order parameter components

Ginzburg-Landau approach - chiral p-wave

order parameter: $\boldsymbol{d}(\boldsymbol{k}) = \hat{z}\boldsymbol{\eta}\cdot\boldsymbol{k} = \hat{z}(\eta_x k_x + \eta_y k_y)$

$$\mathcal{F} = \int dV \, \{a|\boldsymbol{\eta}|^2 + b_1|\boldsymbol{\eta}|^4 + b_2(\eta_x^{*2}\eta_y^2 + \eta_x^2\eta_y^{*2}) + b_3|\eta_x|^2|\eta_y|^2$$

$$+K_1(|\Pi_x\eta_x|^2 + |\Pi_y\eta_y|^2) + K_2(|\Pi_x\eta_y|^2 + |\Pi_y\eta_x|^2)$$

$$+\left[K_3(\Pi_x\eta_x)^*(\Pi_y\eta_y) + K_4(\Pi_x\eta_y)^*(\Pi_y\eta_x) + c.c.\right]$$

$$+K_5|\Pi_z\boldsymbol{\eta}|^2 + (\boldsymbol{\nabla}\times\boldsymbol{A})/8\pi\}$$

and $\boldsymbol{\Pi} = \frac{\hbar}{i}\boldsymbol{\nabla} + \frac{2e}{c}\boldsymbol{A}$

edge currents for chiral phase

Ginzburg-Landau approach - chiral p-wave

order parameter: $\boldsymbol{d}(\boldsymbol{k}) = \hat{z}\boldsymbol{\eta}\cdot\boldsymbol{k} = \hat{z}(\eta_x k_x + \eta_y k_y)$

$$\mathcal{F} = \int dV \, \{a|\boldsymbol{\eta}|^2 + b_1|\boldsymbol{\eta}|^4 + b_2(\eta_x^{*2}\eta_y^2 + \eta_x^2\eta_y^{*2}) + b_3|\eta_x|^2|\eta_y|^2$$

$$+K_1(|\Pi_x\eta_x|^2 + |\Pi_y\eta_y|^2) + K_2(|\Pi_x\eta_y|^2 + |\Pi_y\eta_x|^2)$$

$$+[K_3(\Pi_x\eta_x)^*(\Pi_y\eta_y) + K_4(\Pi_x\eta_y)^*(\Pi_y\eta_x) + c.c.]$$

$$+K_5|\Pi_z\boldsymbol{\eta}|^2 + (\boldsymbol{\nabla}\times\boldsymbol{A})/8\pi\}$$

and $\boldsymbol{\Pi} = \frac{\hbar}{i}\boldsymbol{\nabla} + \frac{2e}{c}\boldsymbol{A}$

cylindrically symmetric bands

$$\frac{1}{3}K_1 = K_2 = K_3 = K_4 \gg K_5$$

Ginzburg-Landau approach - edge currents

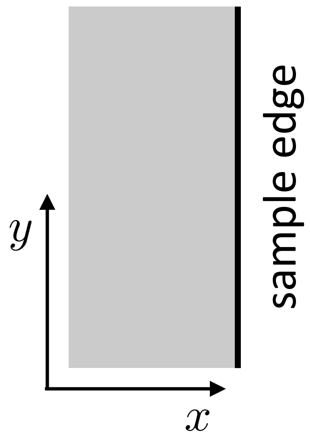

$$K_1|\Pi_x\eta_x|^2 + K_2|\Pi_x\eta_y|^2$$

length scales of order parameter components

$$\xi_x^2/\xi_y^2 = K_1/K_2$$

current density along edge:

$$j_y = \underbrace{16\pi e\hbar\left(K_3|\eta_x|\frac{\partial}{\partial x}|\eta_y| - K_4|\eta_y|\frac{\partial}{\partial x}|\eta_x|\right)}_{\text{driving current}} + \underbrace{\frac{c\lambda^{-2}}{4\pi}A_y}_{\text{screening current}}$$

note: length scales important

Ginzburg-Landau approach - edge currents

$$K_1(|\Pi_x\eta_x|^2 + |\Pi_y\eta_y|^2) + K_2(|\Pi_x\eta_y|^2 + |\Pi_y\eta_x|^2)$$

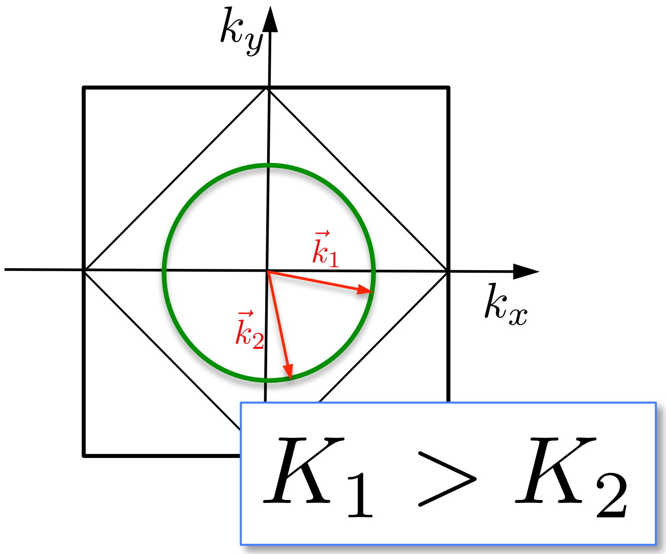

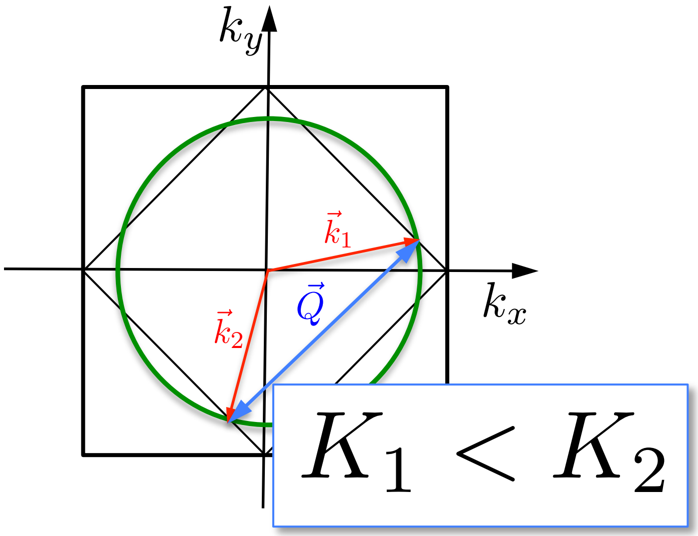

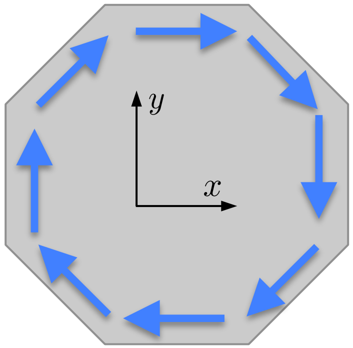

determines
current patter

(specular scattering)

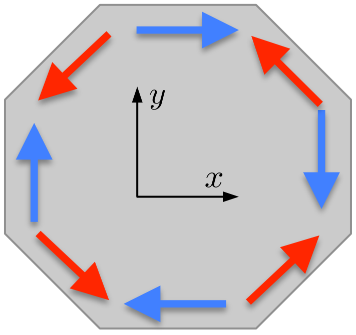

Ginzburg-Landau approach - edge currents

$$K_1(|\Pi_x\eta_x|^2 + |\Pi_y\eta_y|^2) + K_2(|\Pi_x\eta_y|^2 + |\Pi_y\eta_x|^2)$$

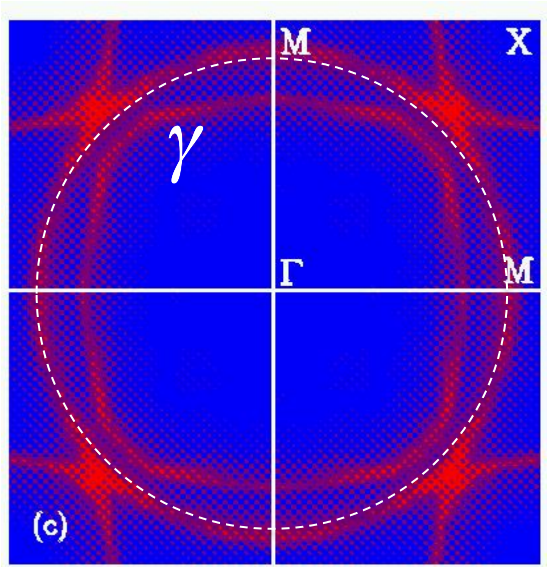

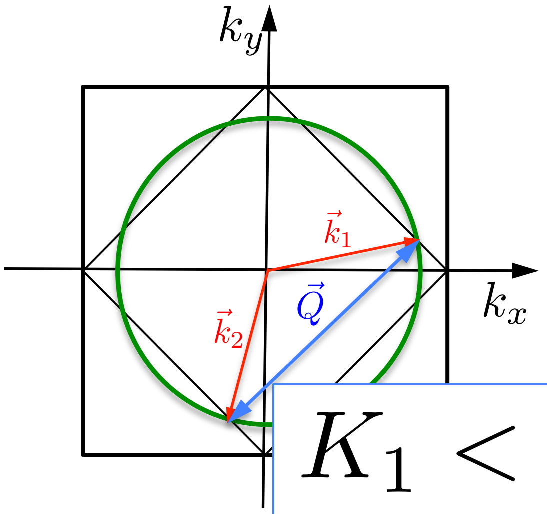

$$K_1 < K_2$$

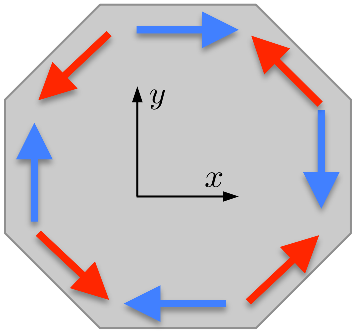

γ-band is most likely dominant and crosses Umklapp diamond

Disk shaped sample

Ginzburg-Landau approach - edge currents

disk shaped sample

S. Etter

current and flux pattern for all surface orientations

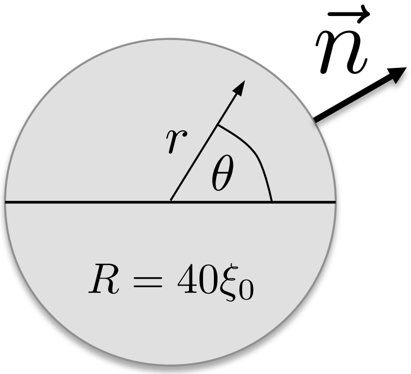

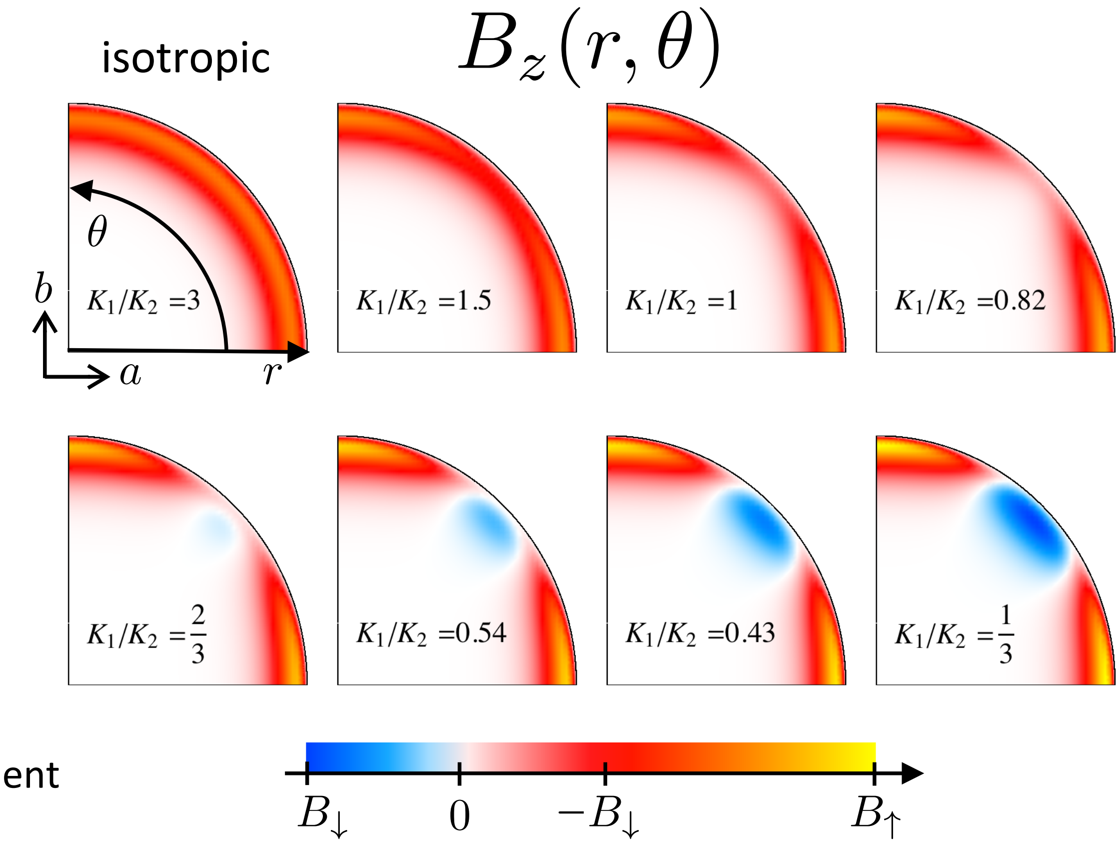

specular scattering

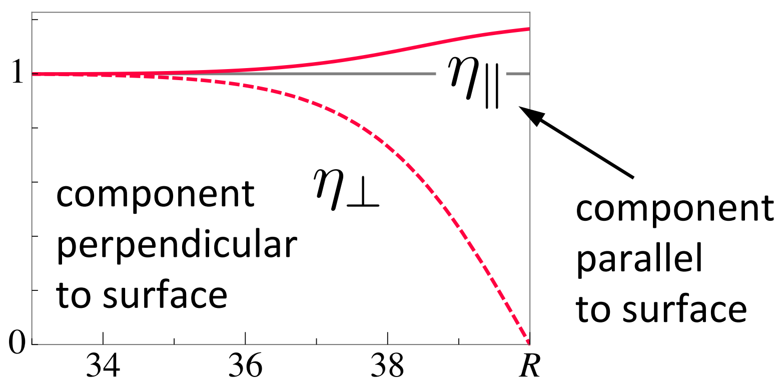

Ginzburg-Landau approach - edge currents

different boundary conditions

specular scattering

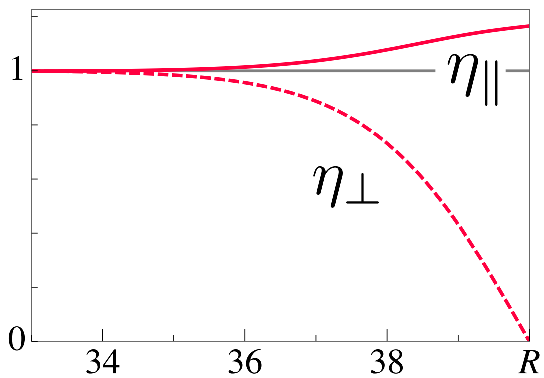

totally pair breaking

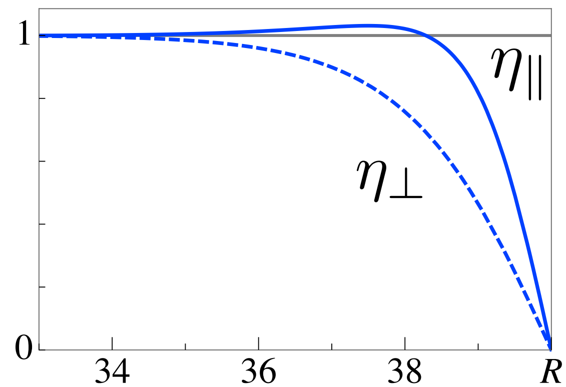

diffuse scattering

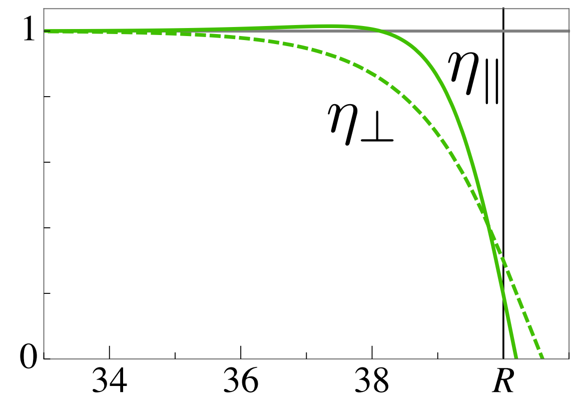

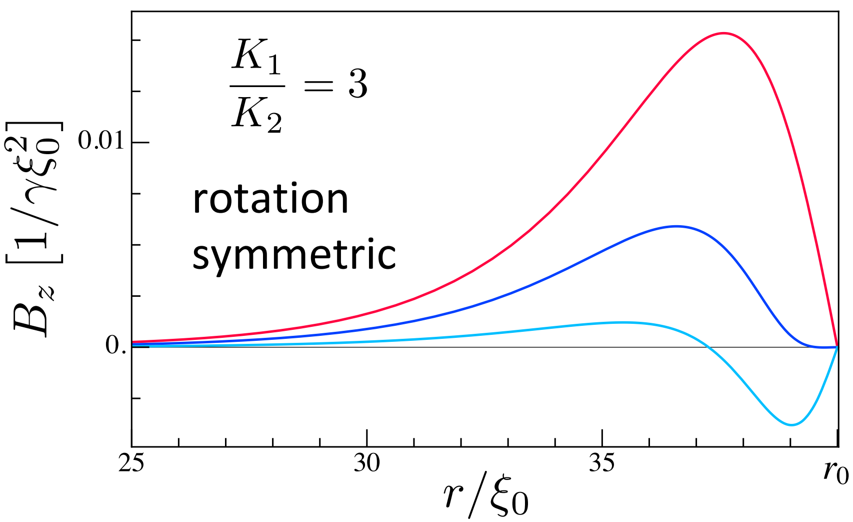

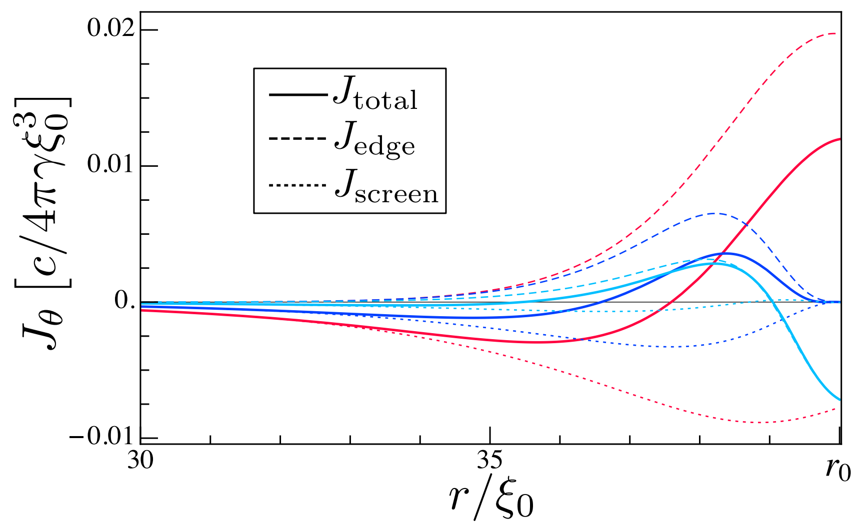

Ginzburg-Landau approach - edge currents

scanning anisotropy and boundary conditions

$B_z(r,\theta)$

isotropic

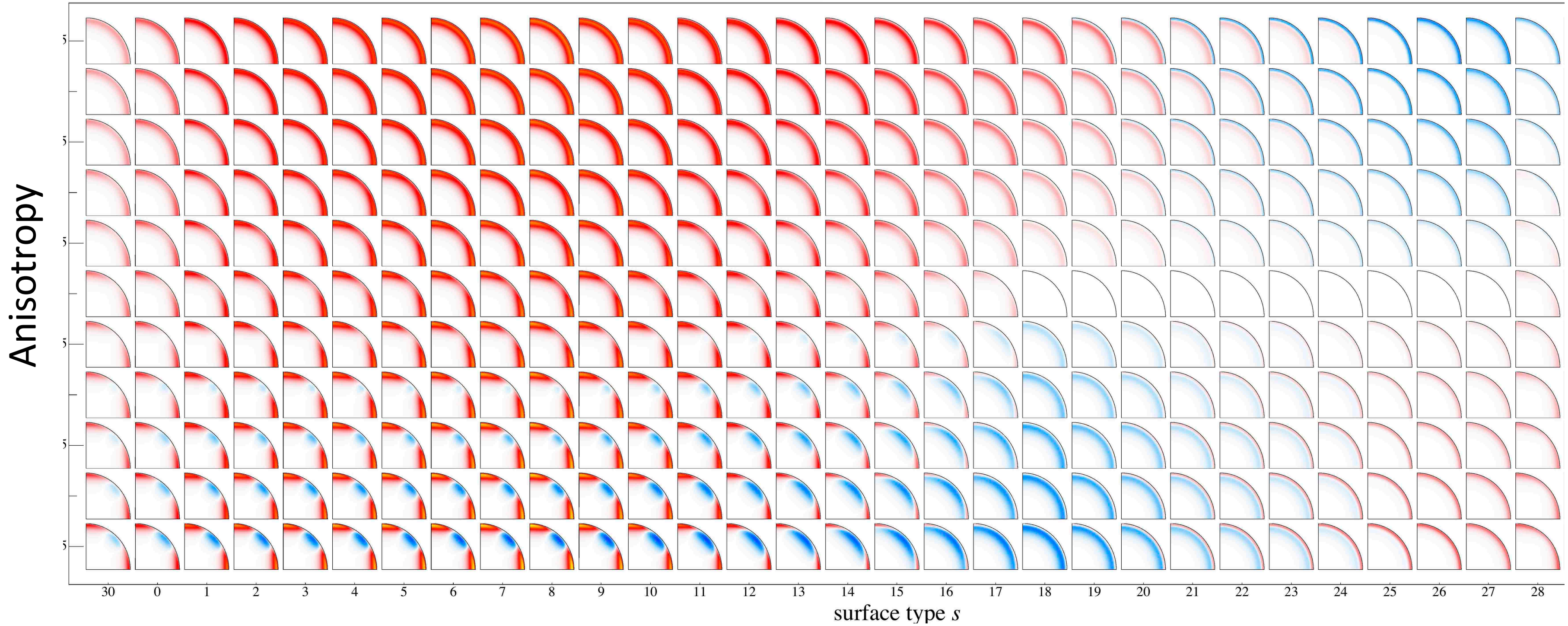

boundary conditions

specular pair breaking diffuse

Ginzburg-Landau approach - edge currents

scanning anisotropy and boundary conditions

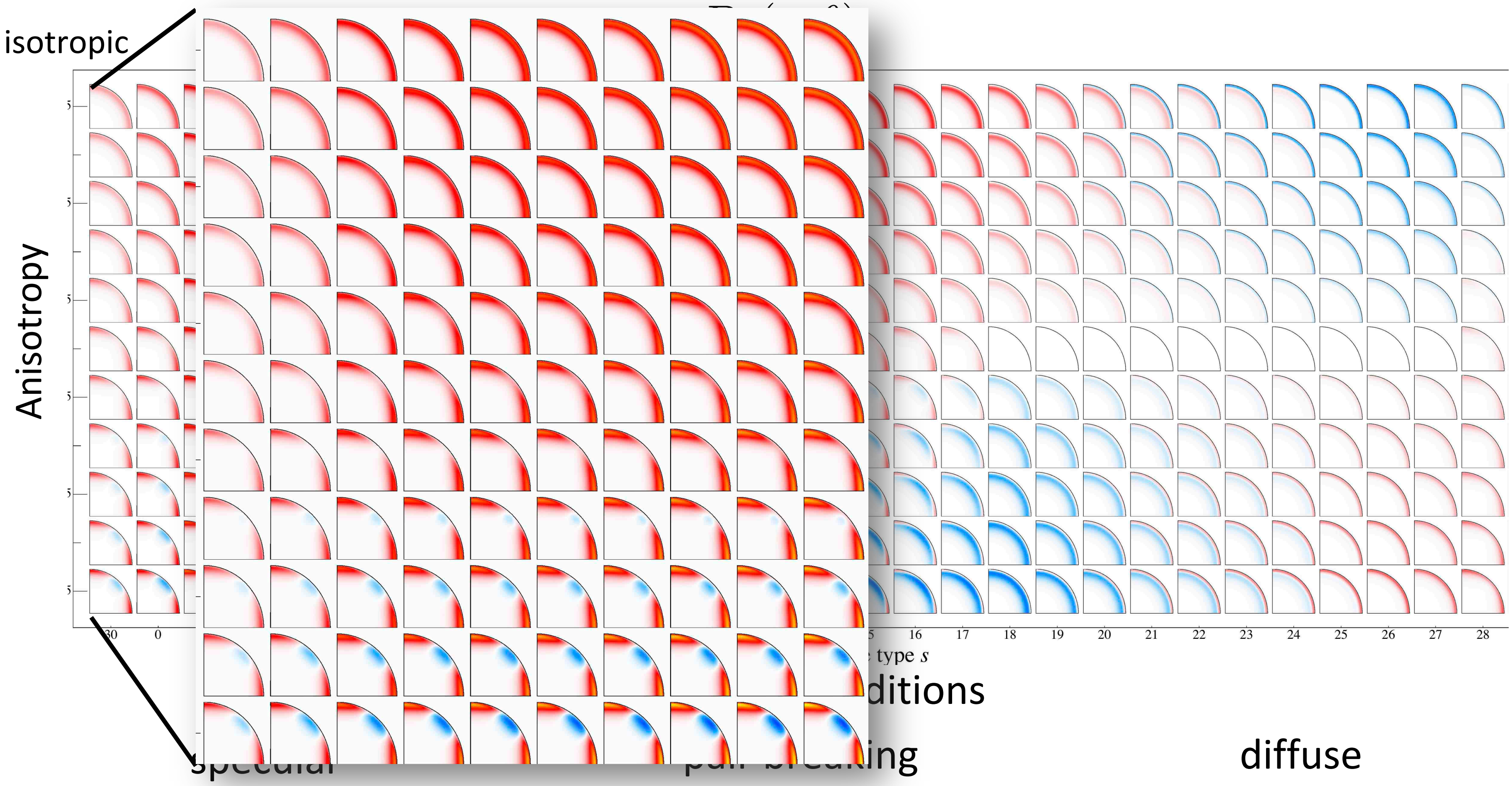

Ginzburg-Landau approach - edge currents

scanning anisotropy and boundary conditions

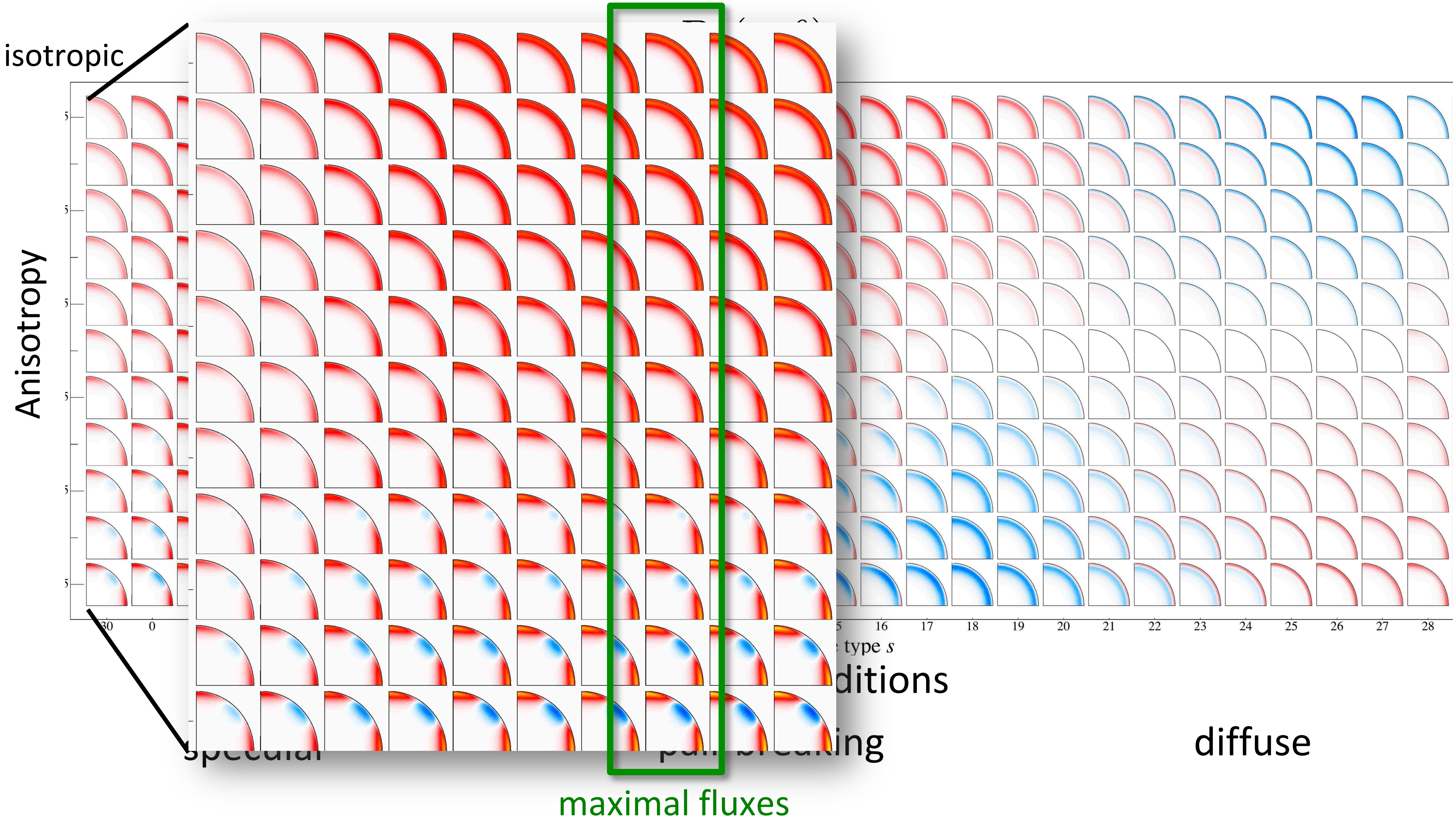

Furusaki, Matsumoto & MS

Ginzburg-Landau approach - edge currents

scanning anisotropy and boundary conditions

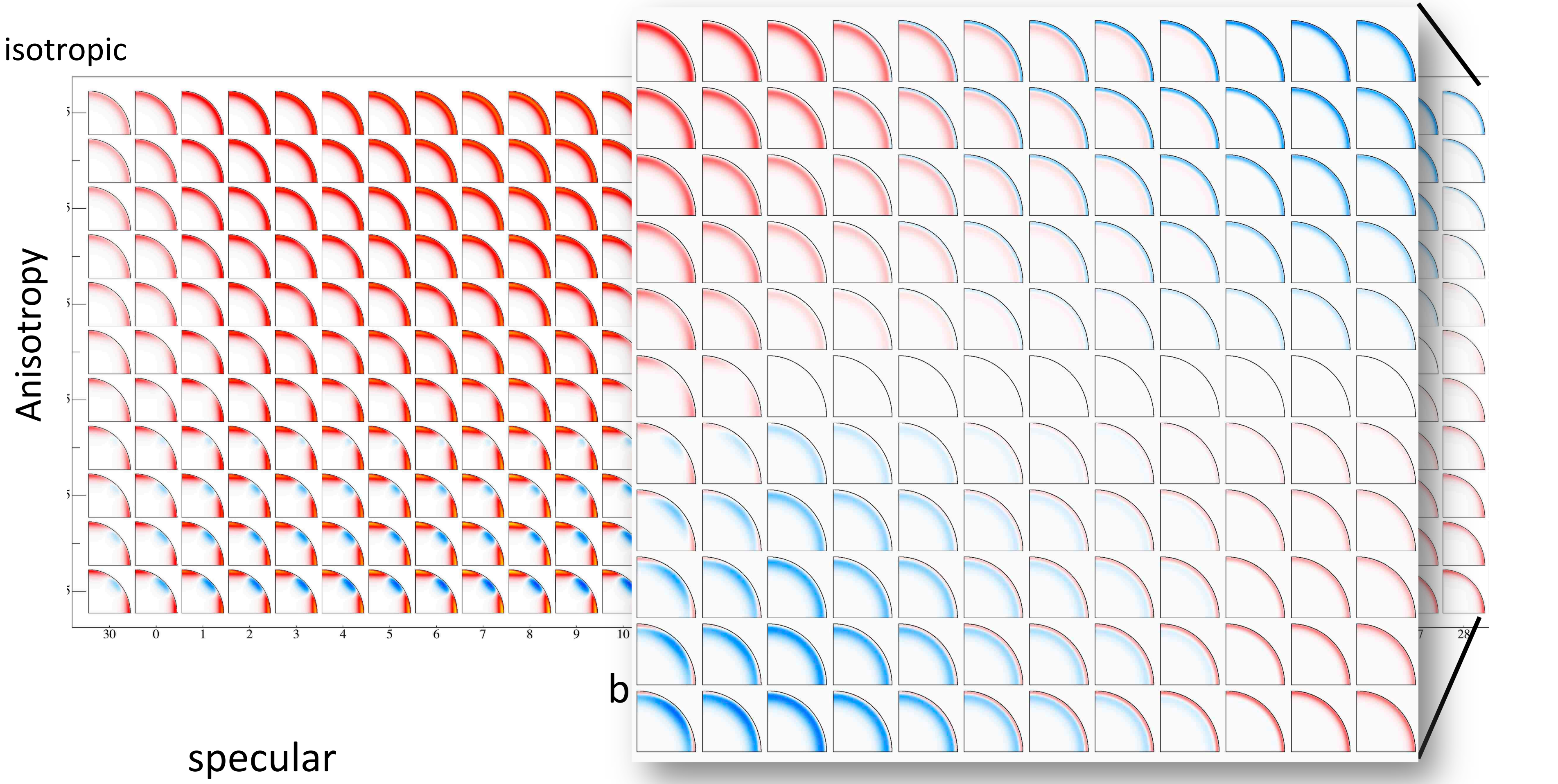

Ginzburg-Landau approach - edge currents

scanning anisotropy and boundary conditions

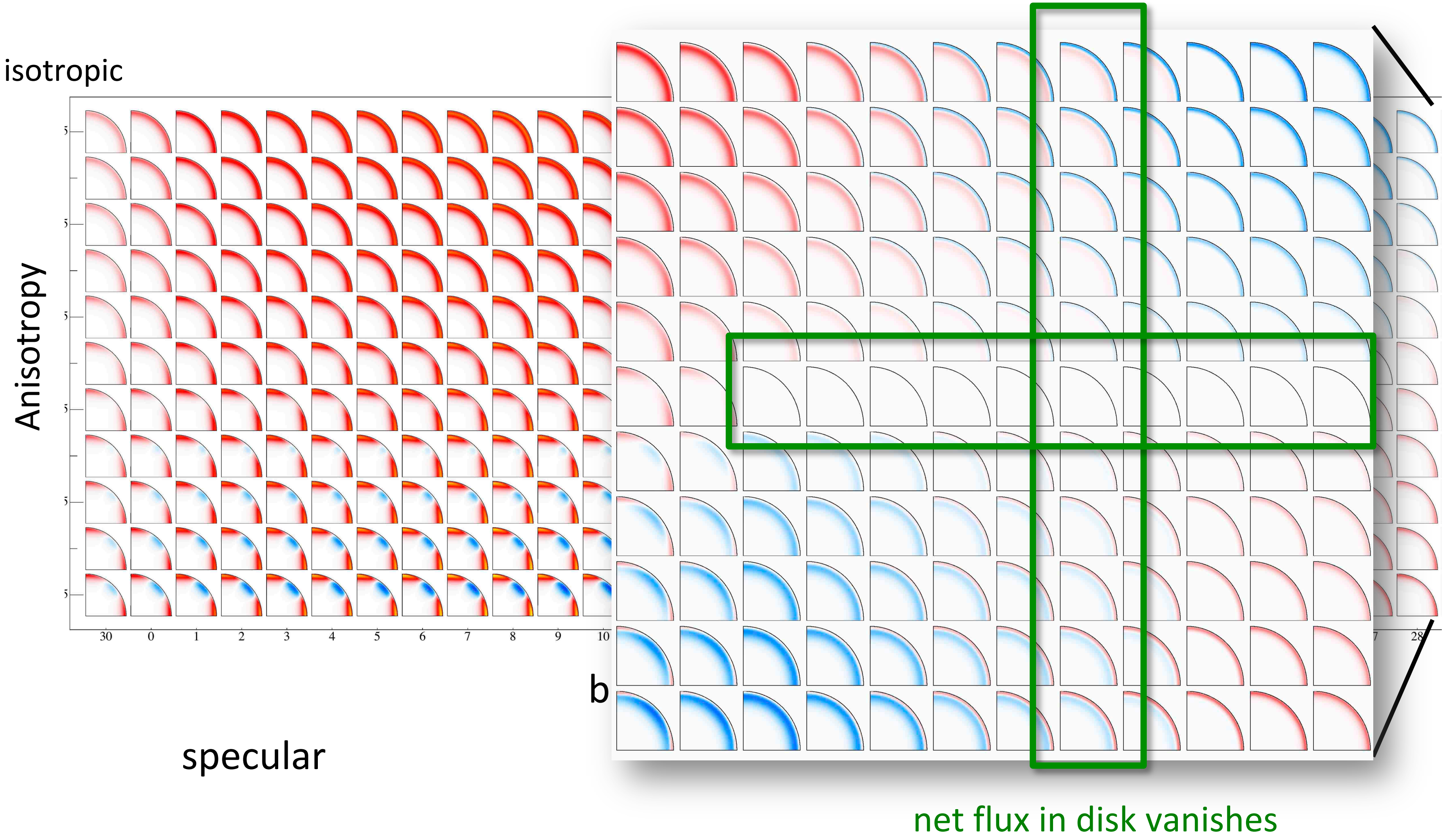

Chiral domain domain walls

Chiral domains and domain walls - chiral p-wave

chiral *p*-wave state

$$\left.\begin{aligned}\Delta^{+}_{\boldsymbol{k}} &= \hat{z}\Delta_0(k_x + ik_y)\\ \Delta^{-}_{\boldsymbol{k}} &= \hat{z}\Delta_0(k_x - ik_y)\end{aligned}\right\}$$

discrete degeneracy 2

2 types of domains

$$\Delta_{\boldsymbol{k}} = \eta_x k_x + \eta_y k_y$$

in-plane domain walls

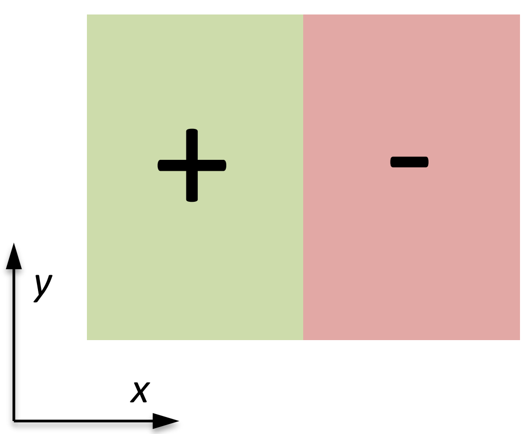

Type 1

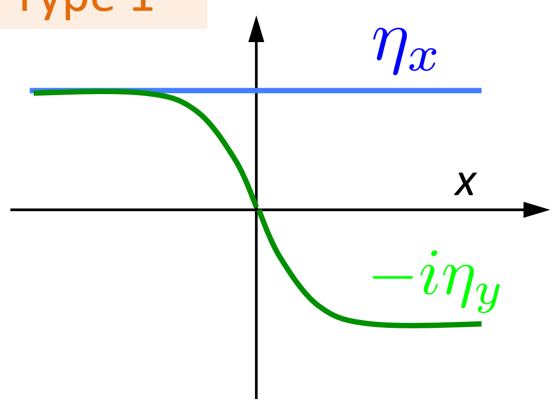

phase switch ~ 0

Type 2

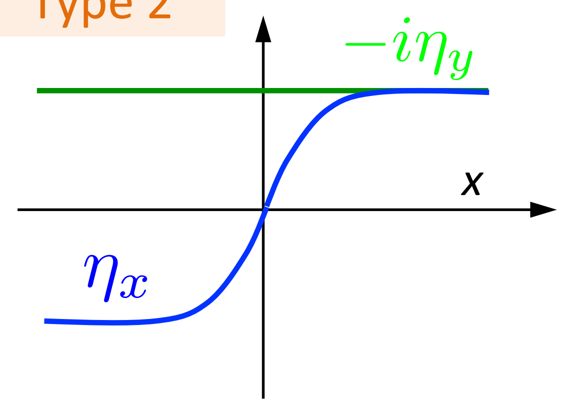

phase switch ~ π

Chiral domains and domain walls - chiral p-wave

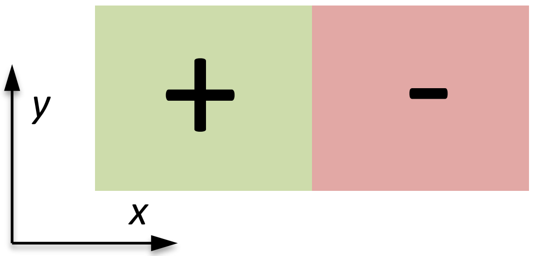

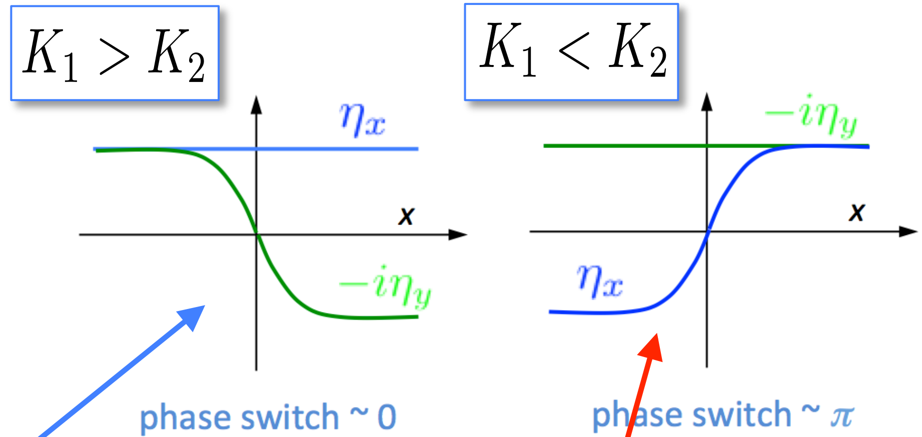

“parabolic band rotation symmetric”

γ-band like Fermi surface in BZ

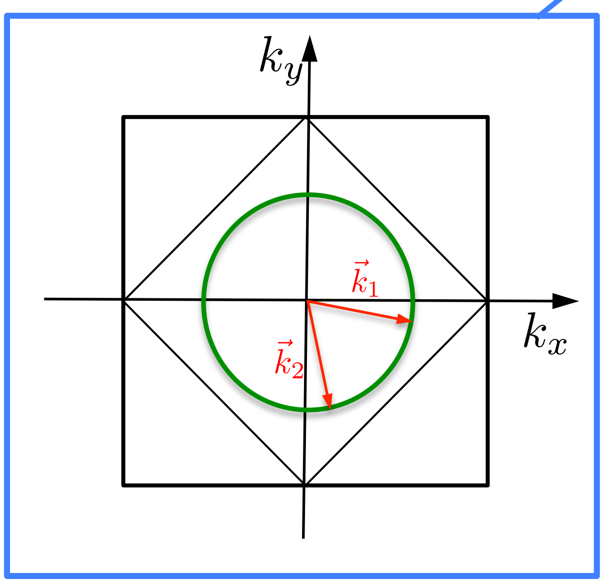

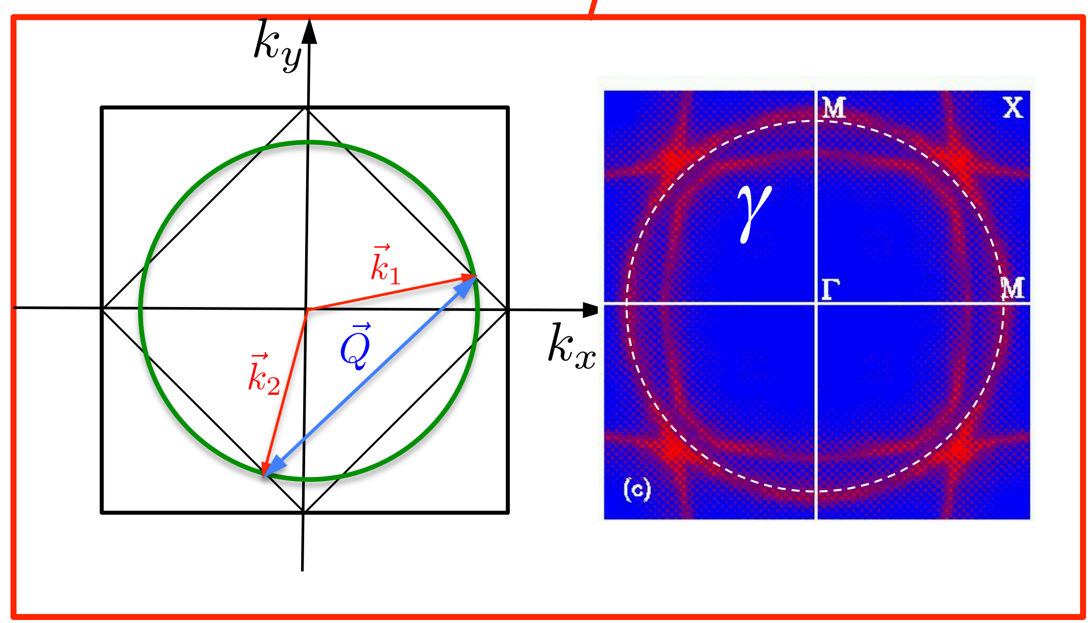

Chiral domains and domain walls - chiral p-wave

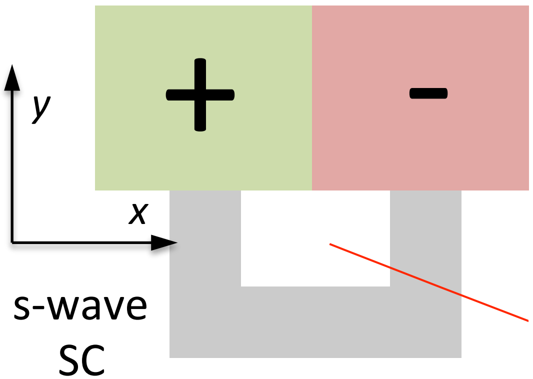

π − loop

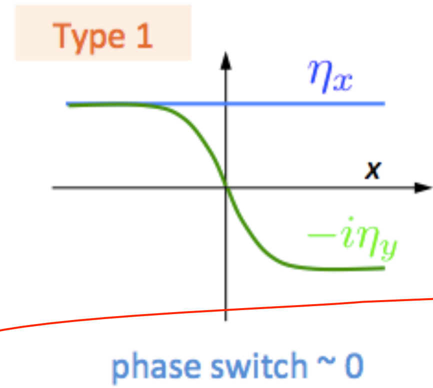

"parabolic band rotation symmetric"

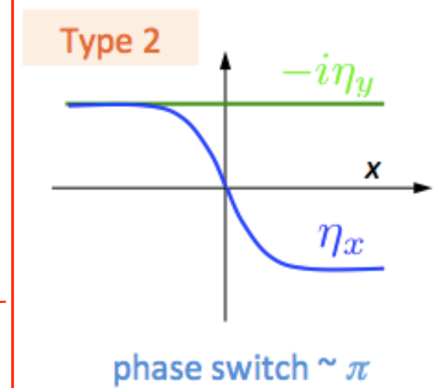

γ-band like Fermi surface in BZ

Josephson coupling

$$J_y \propto Im(\eta_s^*(\boldsymbol{n}\times\boldsymbol{\eta})_z) = |\eta_s||\eta_x|\sin(\phi_s - \phi_x)$$

conservation of total angular momentum

➡ coupling with the x-component

ϕ_x changes by π

through the domain wall

intrinsic phase twist

Chiral domains and domain walls - chiral p-wave

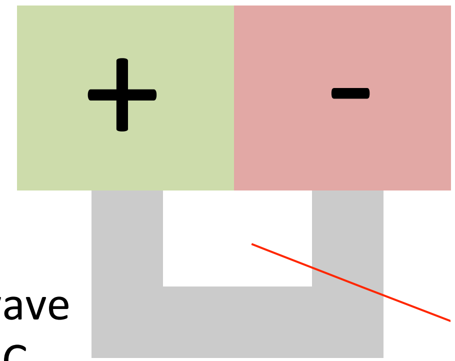

s-wave
SC

$\pi-$loop

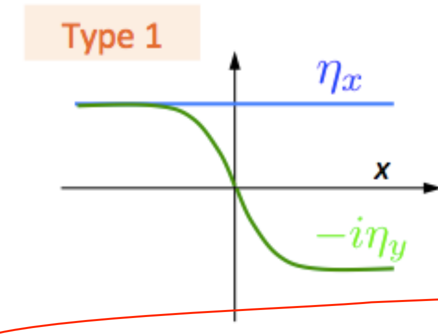

phase switch ~ 0

"parabolic band
rotation symmetric"

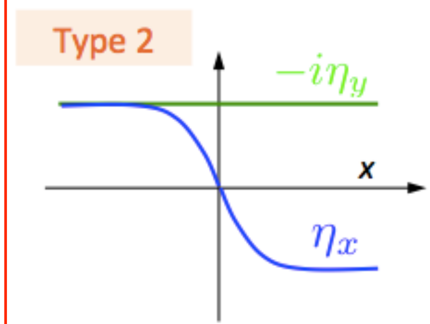

phase switch ~ π

γ-band like
Fermi surface in BZ

narrow s-p-junctions

Sr_2RuO_4-Cu-PbIn

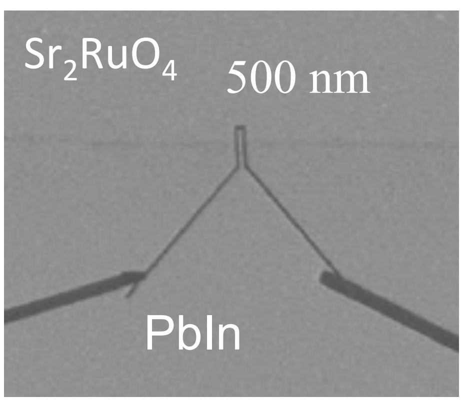

Bahr & van Harlingen

interference pattern

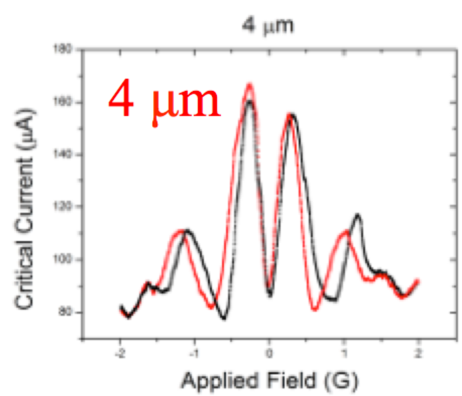

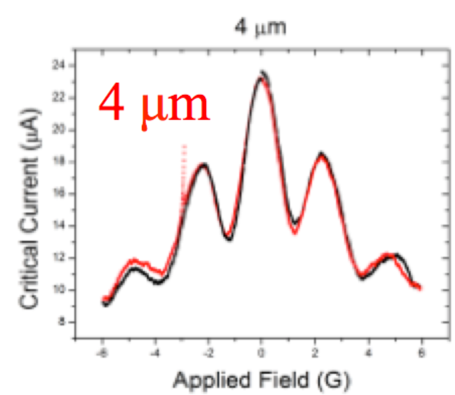

Chiral domains and domain walls - chiral p-wave

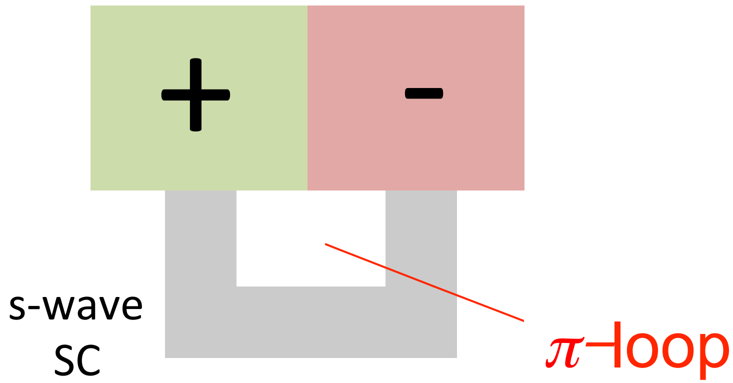

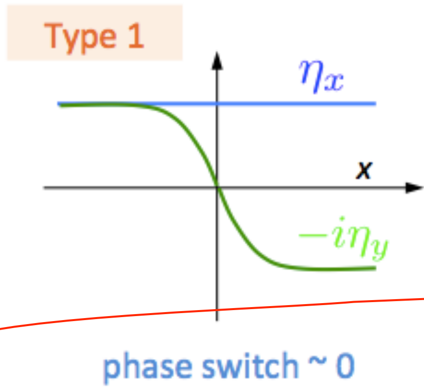

“parabolic band
rotation symmetric”

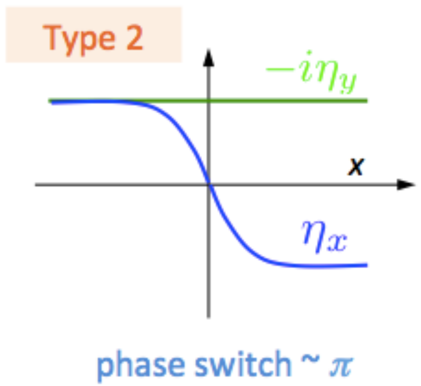

γ-band like
Fermi surface in BZ

extended interface
many domains

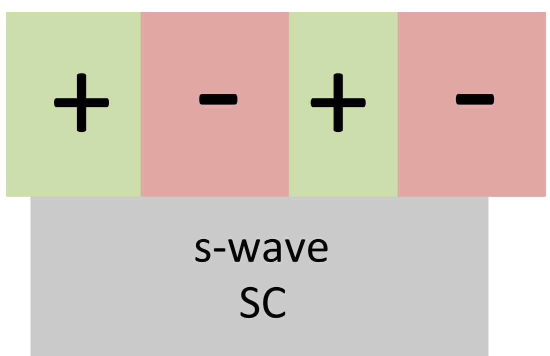

van Harlingen group

Chiral domains and domain walls - chiral p-wave

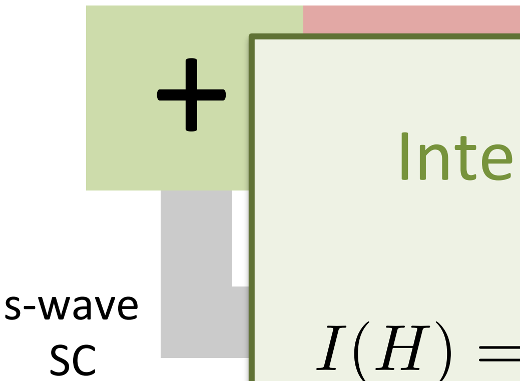

Interference pattern in a magnetic field

$$I(H) = \max_{\phi} \left[\int dx \; j_c \sin\left(\phi - \phi_x(x) - \frac{2\pi H d}{\Phi_0} x \right) \right]$$

rotation symmetric”

Fermi surface in BZ

extended interface

many domains

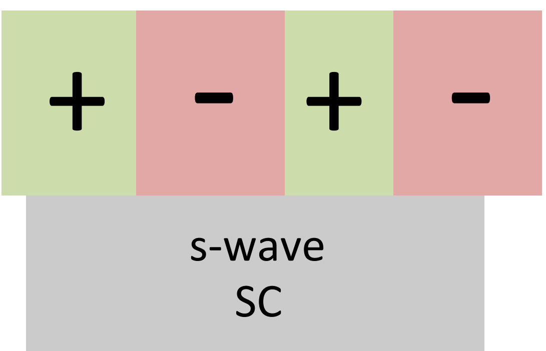

van Harlingen group

irregular – history dependent interference

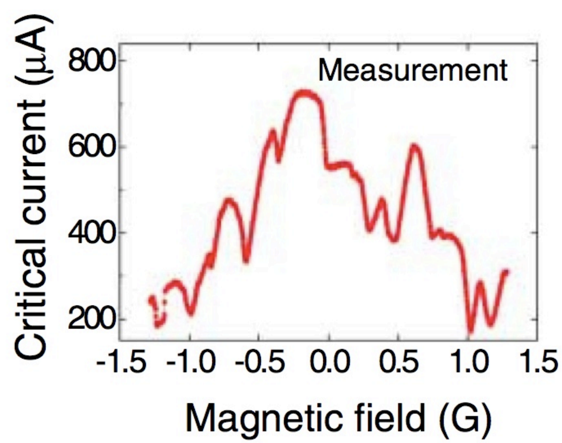

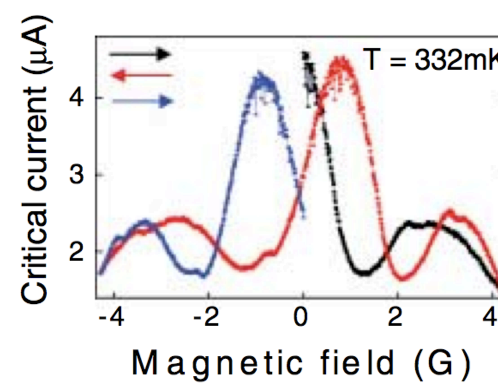

Conclusions

edge currents "invisible"

- supercurrents are not universal
- vanishing would be however accidential

see also C. Kallin group

- note: quantum thermal Hall effect universal

domain walls

- defects of condensate → history dependence
- visible through interference effects